06/29/93

Kinetics and Mechanism of the ClO + CO Reaction: Pressure and Temperature Dependences of the Bimolecular and Termolecular Channels and Thermal Decomposition of Chlorine Peroxide, ClOOCl

Scott Nickolaisen, Randall R. Friedl and Stanley P. Sander*

Jet Propulsion Laboratory

California Institute of Technology

Pasadena, California 91109

Submitted to the Journal of Physical Chemistry

NASA/NRC Resident Research Associate

* Author To Whom Correspondence Should Be Addressed

Abstract

The kinetics and mechanism of the ClO -1 ClO reaction and the thermal decomposition of ('100('1" were studied using the flash photolysis/long path ultraviolet absorption technique. Pressure and temperature depender ices were determined for the late coefficients for the bimolecular and termolecular reaction channels, and for the thermal decomposition of ClOOCl. In order to determine channel specific rate coefficients and to minimize complications associated with secondary chemistry, the reaction was studied over wide ranges of initial reactant stoichiometry and temperature. The rate coefficient for the termolecular association channel in the low pressure limit

$$ClO + ClO - \xrightarrow{M} ClOOCl \qquad (1)$$

with N_2 as a third body was measured over the temperature range 195 - 390 K and resulted in $k_{1,N_2}(T) = (1.22 \pm 0.15) \times 10^{-33} \exp\{(833 \pm 34)/T\}$ cm^6 molecule^{-1} s^{-1} (2 σ error bounds). The 300 K rate coefficient for reaction 1 was measured for a number of bath gases. The results are $k_{1,M}$(x 10^{-32} cm^6 molecule^{-2} s^{-1}) = 0.99 ± 0.05, 1.24 ± 0.09, 1.71 ± 0.06, 2.60 ± 0.17, 3.15 ± 0.14 and 6.7 ± 3.6 for He, O_2, Ar, CF_4, SF_6 and Cl_2, respectively. The effective collision efficiency for M = Cl_2 is very large and is likely due to a chaperone mechanism. Below 250 K, the reaction was in the falloff regime between second- and third-order kinetics. From the falloff data, the rate constant in the high pressure limit, k_∞^{300}, was estimated to be (6 ± 2) x 10^{-12} cm^3 molecule^{-1}s^{-1}. The Arrhenius expressions for the three bimolecular channels,

$$ClO + (:lo- \quad) Cl_2 + O_2 \qquad (2)$$

$$) ClOO + Cl \qquad (3)$$

$$) OClO + Cl \qquad (4)$$

over the temperature range 260390 K are $k_2(T) = (1.01 \pm 0.12) \times 10^{-12} \exp\{-(1590 \pm 100)/T\}$ cm^3 molecule^{-1}s^{-1}, $k_3(T) = (2.98 \pm 0.68) \times 10^{-11} \exp\{-(2450 \pm 330)/T\}$ cm^3 molecule^{-1} s^{-1} and $k_4(T) = (3.50 \pm 0.31) \times 10^{-13} \exp\{-(1370 \pm 150)/T\}$ cm^3 molecule^{-1} s^{-1}. These expressions lead to a value of (1.64 ± 0.35) x10^{-14} cm^3 molecule^{-1}s^{-1} for the overall bimolecular rate constant (k_2+k_3+k_4) at 298 K. The rate coefficient expression for ClOOCl thermal (lee.(,ll[])c,siti(,l] was determined to be $k_{-1}(T) = (9.81 \pm 1.32) \times 10^{-7} \exp\{-(7980 \pm 320)/T\}$ cm^3 molecule^{-1} s^{-1} over the range 260 - 310 K. From a Third Law analysis using equilibrium constants derived from measured values of k_1 and k_{-1}, the enthalpy of formation ($\Delta H^o_f(298)$) of ClOOCl was determined to be 30.5 ± 0.7 kcal/mol"]. The equilibrium constant expression from this analysis is $K_{eq}(T) = (1.24 \pm 0.18) \times 10^{-27} \exp\{(8820 \pm 440)/T\}$ cm^3 molecule^{-1}. From the observed activation energy for reaction 4 and the literature activation energy for reaction -4, the OClO enthalpy of formation was calculated to be 22.6 ± 0.3 kcal 1110]].

Introduction

In the last few years, there has been considerable interest in reactions that proceed over complex potential energy surfaces. Because long-lived collision complexes may form in these reactions, the experimental rate coefficients may show significant pressure dependences, negative temperature dependences (which vary with pressure) and product distributions which depend on the pressure and temperature.

The self-reactions of halogen monoxide radicals are interesting examples of reactions which proceed via collision complexes. Of the ten reactions of the type

$$XO + XO \rightarrow \text{products}$$

$$XO + YO \rightarrow \text{products}$$

where X,Y = F, Cl, Br, I, there are experimental data on five (FO + FO, ClO + ClO, ClO + BrO, BrO + BrO and IO + IO). Of these, the ClO + ClO reaction,

$$ClO + ClO \rightarrow ClOOCl \quad (1)$$

$$ClO + ClO \rightarrow Cl_2 (^1\Sigma, 31) + O_2 \quad (?)$$

$$\rightarrow Cl + ClOO \quad (3)$$

$$\rightarrow Cl + OClO \quad (4)$$

is perhaps the most complex because of the multiplicity of channels leading to stable products. The association (termolecular) channels form ClOOCl and ClOClO via surfaces with essentially no potential barrier. The corresponding bimolecular product channels proceed through loose transition states to give Cl + ClOO and Cl + OClO across surfaces with a significant potential barrier. Finally, the molecular elimination channel produces Cl_2 ($^1\Sigma$, $^3\Pi$) + O_2 through a tight transition state originating in the ClOOCl intermediate. Because of the complexity of this system, the experimental description of the pressure and temperature dependences of the product branching ratios is far from complete.

The ClO + ClO reaction also plays an important role in atmospheric chemistry. Cl atoms, which are produced from the photochemical degradation of chlorofluorocarbons, react with O_3 to produce ClO radicals from the reaction,

$$Cl + O_3 \text{ ----- } \rightarrow ClO + O_2$$

Under normal stratospheric conditions, the self-reaction of ClO radicals cannot compete with reactions such as

$$O + ClO \rightarrow Cl + O_2$$

and

$$BrO + ClO \rightarrow Br + ClOO$$

as an important rate-limiting step in the catalytic destruction of O_3. In the highly perturbed conditions present in the polar stratosphere, however, where catalytic processes on the surfaces of polar stratospheric cloud particles can result in the re-partitioning of inorganic chlorine into predominantly active forms, the following cycle may play an important role in O_3 destruction:

$$ClO + ClO \xrightarrow{M} ClOOCl$$

$$ClOOCl + h\nu \longrightarrow Cl + ClOO$$

$$ClOO \xrightarrow{M} Cl + O_2$$

$$2(Cl + O_3 \rightarrow ClO + O_2)$$

$$\text{Net:} \quad 2O_3 \rightarrow 3O_2$$

Since the ClO + ClO reaction is partially rate-determining in this cycle (the photolysis of ClOOCl also plays a role), it is important to determine the temperature and pressure dependences of the rate coefficients under atmospheric conditions, During the day, photolysis of ClOOCl is much faster than unimolecular decomposition. Under nighttime conditions, the removal of ClOOCl is most likely dominated by thermal decomposiiton and the rate of this process must be known to calculate the partitioning between chlorine-containing species. Because thermally stabilized ClOOCl has at least three unimolecular decomposition channels (ClO + ClO, Cl + ClOO, $Cl_2 + O_2$), and these channels have different atmospheric consequences under nighttime conditions, it is also important to establish the thermal decomposition branching ratios under atmospheric conditions.

The ClO + ClO reaction has been studied extensively by direct and indirect methods for several decades. Early work on the photolysis of Cl_2-O_3 mixtures [1,2] suggested the importance of the ClO + ClO reaction in propagating, the chain destruction of O_3. The first direct studies of reaction 1 did not come about until the development of the flash photolysis technique and the subsequent identification of the ultraviolet absorption spectrum of ClO.[3,4] Since these early studies, rate coefficients for reaction 1 have been measured using several kinetic techniques including flash photolysis-ultraviolet absorption,[5-8] discharge flow-ultraviolet absorption,[9-11] discharge flow-mass spectrometry[12] and molecular modulation-ultraviolet absorption,[13-18]

Rate coefficients for the termolecular component have been obtained by Basco and Hunt,[6] Hayman *et al.*,[17] Sander *et al.*[7] and Trolier *et al.*[8] The latter two studies were carried out in the temperature range relevant to the polar stratosphere and are in reasonably good agreement,

although Trolier *et al.* observed non-m-o intercepts in the rate coefficient falloff curves which were not observed by Sander *et al.*

By comparison, the bimolecular channels arc poorly understood. Recent results for the overall bimolecular rate coefficient at 298 K ($k_2+k_3+k_4$) have ranged over a factor of about four, and there is only one study of the temperature dependence of this parameter. 'J'here are no temperature dependence studies of the branching ratios for the bimolecular channels. Steady-state photolysis studies of the chlorine-photoscnsitizcci decomposition of ozone have consistently given values of about 6 for the quantum yield for ozone destruction in N_2 bath gas at 298 K, implying a branching ratio of about 2 for the ClOO + Cl channel relative to the $Cl_2 + O_2$ channel [19] '1'here arc no time-rcsolvcci studies of the branching ratios in M: N2 with which to compare these results.

1 {equilibrium constants for the reaction

$$2ClO \langle^{M}\rangle ClOOCl$$

have been measured by Basco and 1 lunt[6] and Cox and 1)erwent[15] at room temperature anti by Cox and 1 layman 20 over the temperature range 233 - 303 K. These results arc in reasonable agreement and lead to a calculated O-O bond (dissociation energy of 17.3 kcal mol^{-1} assuming ClOOCl to bc the predominant form of the ClO dimer.

in this paper we present the results of an extensive study of the ClO + ClO reaction with the goal of characterizing the rates and mechanism of both the bimolecular and termolecular channels over a wide range of temperature and pressure using several different collision partners. Evidence is presented for the existence of a imp)-livcci $ClO{\cdot}Cl_2$ complex which greatly enhances the apparent rate of the recombination channel. Results arc also presented on the rate of thermal decomposition of C1OOCI.

Experimental

'l-he experiments described in this paper were carried out using the flash photolysis/ultraviolet absorption technique. The apparatus has been described in detail previously.[21] The flash lamp/reactor is a unit consisting of four concentric Pyrex tubes, approximately 1 m long, comprising the reaction cell (1 in i.d.), photolyzing light filter, xenon flash lamp and cooling/heating jacket. The ccl] was operated in the continuously flowing mode, with al l reagent and carrier gas flows being measured with calibrated mass flow meters. The analytical light source was a 150 W xenon arc lamp which was collimated and 'coupled into the reaction cell through 8-pass White-type optics with external mirrors. The optical path length was 720 cm. The exit beam was transferred via a switching mirror to a 0.32 m focal length spectrograph (150 μm slit width, 0.18 nm resolution) equipped with a 1024 channel optical

multichannel analyzer (OMA) for the detection of C1O and OC1O, or to a 0.5 m monochromator (150 μm slit width, 0.13 nm resolution) and photomultiplier for the detection of ClO and Cl_2O. The photomultiplier output was amplified, low-pass filtered and digitized with a signal averager interfaced to a microcomputer.

in experiments which used the photomultiplier, ClO radicals were monitored by their absorption at the peak of the 12-0 Ω= 3/2 subband (A< X) at 275.5 nm. in the OMA experiments, five vibrational bands (1 O-O, 11-O, 12-O, 13-0 and 14-O) were monitored over the wavelength range 270 - 280 nm. OClO was monitored using the OMA over the wavelength range 340-400 nm which encompassed seven vibrational bands [a(6), a(7), a(8), a(9), a(10), a(11) and a(12)]. The OMA was normally operated in the time-resolved mode.[21] in this mode, up to 500 sweeps could be recorded per flash with each sweep consisting of a 1024 channel spectrum with a minimum 16 rns averaging time. in a few experiments, the OMA time resolution was increased by operating the OMA with a reduced number of channels (200 channels, 4 ms resolution), which also reduced the spectral coverage. OClO and ClO spectra from the OMA were processed by first coadding and converting to absorbance the spectra from 5 to 20 successive flashes. Spectra were convolved with a 7 point triangular kernel to match the exit slit function of the spectrograph. Because of the formation and removal of species such as Cl_2O and ClOOCl which have slowly varying continuum absorption which overlap the species of interest, it was necessary to eliminate time-varying baseline offsets. This was accomplished by subtracting from the smoothed spectrum a third-order polynomial obtained from a curve fit to the spectrum. Absolute ClO and OClO concentrations were obtained by fitting each observed spectrum to calibrated literature spectra using the conjugate gradient method. For these experiments, the OMA was preferred over the PMT because of several important advantages. Because both C1O and OClO have absorption spectra with distinguishing vibrational band features, retrieval of these features provided a means to discriminate against time-varying baseline shifts from continuum absorbers. This was particularly important for the high temperature experiments with excess Cl_2O because of the effect of chain Cl_2O removal on the ClO absorption baseline. The second benefit stems from the OMA multiplex advantage which arises from the use of 1024 separate detectors in the focal plane. This results in a signal-to-noise ratio improvement of more than a factor of 10 over the photomultiplier. The detection limit for both ClO and OClO using the OMA was about 2 x 10^{10} molecule cm^{-3}.

1 :xperimental signals were converted to absorbance units using Beer's Law,

$$A = -N\sigma l = -\ln\{I/I_o\}$$

where N is the species concentration, σ is the absorption cross section and 1 is the pathlength. 1_o was determined from the pre-flash signals for PM"]' and OMA data recorded at higher temperatures (T $\geq$ 250 K). The signal as $t \rightarrow \infty$ was used as 1_o for low temperature (T < 250 K)

PMT data. For I'MT' data collected at 275.5 **nm,** four species (C1O, Cl_2O, C1OOC1, Cl_2) have significant absorption with the following absorption cross sections at 298 K: σ_{ClO} = 8.4 x 10-'8 cm^2,[21] σ_{Cl_2O} = 1.24 x 10-18 cm^2,[22] $C J_{ClOOCl}$ = 2,45 x 10^{-18} cm^2,[23] and σ_{Cl_2} = 2.19 x 10-20 cm^2.[24] The measured absorption cross section of ClO shows a temperature dependence,[21] however, the variation of σ_{ClO} over the temperature range of the excess chlorine atom experiments (260 K ≤ T ≤ 400 K) is less than 7°/0 *so* no correction was made for this variation in the fitting routine. At 195 K, the lowest temperature of the excess Cl_2O PMT data, the ClO cross section is extrapolated to be 10.6 x 10-] $^8cm^2$.

OMA rcfcrencc spectra were obtained by coadding 1000 spectra collected under conditions which maximized either the C1O or OClO signals. For C1O, 100 spectra at a time resolution of 4 ms were collected immediately following the flash when the ClO concentration was greatest. This cycle was repeated ten times to achieve a total of 1000 averaged spectra. The absolute ClO concentration of the resulting spectrum was calculated by comparing the absorbance difference between successive maxima and minima of the absorption spectrum to the relative cross section differences of the same maxima and minima determined previously.2] By using relative cross sections between maxima and minima of the absorption spectrum instead of absolute cross sections, possible errors caused by background absorption from Cl_2O, Cl_2, or ClOOCl were minimized. For OClO, 1000 spectra were collected at a time resolution of 20 ms beginning 5 seconds following the flash. This allowed OC1O formation to reach a maximum. This rcfcrencc spectrum was converted to absolute concentration in the same manner as described for C1O by comparison of the relative absorbances to the OClO cross sections measured by Wahner *et al.*[25] Because of the improved signal-to-noise of the OMA data which allowed the rate coefficients to bc determined rnorc precisely, the temperature dependences of the ClO and OClO absorption cross sections were used when calculating the absolute concentration of the rcfcrencc spectrum. For ClO, the expression used to calculate the cross section at a given temperat urc was

$$\sigma_{ClO}(T) = \sigma_{ClO}(298)\{ 1.011- 104.9/T+ 30330/'1'^2\}$$

where $0_{C10}(298)$ = 8.4 x $10^{-]8}$ cm^2 $molecule^{-1}$ is the cross section at 275.5 nm. This expression was derived by fitting the C1O cross sections reported by Sander *et al.*[21] versus 1/1' to a quadratic equation. The usc of a quadratic equation dependent on inverse temperature was somewhat arbitrary and was chosen because it provided the best visual interpolation of the data.]n the case of OC1O, the expression was

$$\sigma_{OClO}(T) = \sigma_{OClO}(296)\{ 1.733- 0.00248"1^{-}\}$$

where $0_{0C10}(296)$ = 1.275 x 10-17 cm^2 $molecule^{-1}$ is the cross section for the a(1 1) line. This expression was derived by fitting the a(1 1) cross sections reported in ref. 26 versus temperature to a straight line.

The mechanism employed in the study of the ClO + C1O reaction used the photolysis of Cl_2-Cl_2O mixtures at wavelengths longer than 300 nm (Pyrex cutoff). In this system, C1O radicals were formed by the reactions

$$Cl_2 + h\nu \longrightarrow 2Cl$$

$$Cl + Cl_2O \longrightarrow ClO + Cl_2 \qquad (5)$$

and to a minor extent from the photolysis of Cl_2O,

$$Cl_2O + h\nu \longrightarrow Cl + ClO.$$

As discussed in the Results section, conditions for reaction 5 were employed such that either Cl or $C1_20$ were present in excess. In either case, the production of ClO typically took place on a time scale three to four orders of magnitude faster than its removal. The exception to this condition occurred when 0_2 was used as the buffer gas. in this case, ClO was also formed by the reactions

$$Cl + O_2 \xrightarrow{M} Cloo$$

$$c1 + ClOO \longrightarrow 2ClO.$$

which occurred on a longer time scale. This formation mechanism will be discussed below.

Cl_2O was prepared by the method of Cady[7] Residual chlorine from the synthesis was removed by distillation at -112 °C. $C1_20$ was introduced into the flash photol ysis cell by flowing helium at 5 psia through a bubbler containing the pure liquid at -78 ‘C. Ultra-high purity chlorine, helium, argon, nitrogen, oxygen, CF_4 and SF_6 were used as received.

Results

The primary objectives of this work were to measure the rate coefficients for all of the known bimolecular and termolecular channels of the C1O + ClO reaction and to measure rate coefficients for the unimolecular decomposition of C1OOCI to 2C1O over as wide a range of pressure and temperature as possible. The major difficulty in determining channel-specific rate parameters for the C1O self-reaction arises from the rapid regeneration of C1O from Cl and C1OO radicals produced in reactions 3 and 4. in addition, at temperatures above about 250 K, the thermal decomposition of C1OOC1 back to C1O plays a major role in determining the C1O time dependence. These regeneration mechanisms complicate the kinetic analysis of both the primary C1O decay and the formation of OClO and have been a major source of uncertainty in previous studies.

Mechanism. The complete set of reactions considered in the kinetic analysis is given in ‘l’able 1. For completeness, the mechanism explicitl y considers all the known reactions that

involve ClO formation and removal, reactions of C1OO, OClO and C1OOCI and Cl termination. However not all these reactions are important under all conditions. The stoichiometric and temperature regimes in which individual reactions play an important role are indicated in Table 1. Most of the rate coefficients were taken from the NASA kinetics data evaluation[26] including the expressions for k_{-1} and k_{-7} which were derived by combining the tabulated temperature dependent expressions for the reverse reactions and equilibrium constants. Flow through the cell was also included in the mechanism and was modeled by a single exponential function with a time constant, τ_{flow}. l-he value of τ_{flow} was in the range 0.1-0.01 s^{-1}. The effect of flow on the observed signals was minimal as the residence time of reactants and products in the cell was adjusted to bc 5-20 times longer than the time interval over which useful data was acquired.

For the experiments which employed excess Cl, it was necessary to estimate the time dependence of the chlorine atom concentration. Cl loss can occur by the direct recombination react ion,

$$Cl + Cl \xrightarrow{M} Cl_2 \qquad (9)$$

and also by ClO catalysis,

$$cl + ClO \xrightarrow{M} Cl_2O \qquad (8)$$

$$cl + Cl_2O \longrightarrow Cl_2 + ClO \qquad (5)$$

$$\text{Net: } Cl + Cl \xrightarrow{M} Cl_2$$

For the latter mechanism, reaction 8 is the rate limiting step. Since the Cl + ClO recombination reaction has not been studied experimentally, an estimate of the low-pressure limiting rate constant was made using the method developed by Trot.[28] A value of 6 x 10-32 cm^6 $molecule^{-2}$ S-l was estimated at 298 K.

In order to minimize the complications arising from secondary chemistry, the reaction was studied in three different regimes of initial reactant stoichiometry (Cl_2O:Cl) and temperature. These regimes were 1) excess Cl_2O, $T \leq 250$ K, 2) excess Cl, 250 K $\leq T \leq$ 400 K and, 3) excess Cl_2O, 250 K $\leq T \leq$ 400 K. The ranges of reactant concentrations for each of these kinetic regimes is summarized in Table II. The experimental conditions as well as the mechanisms used in the analysis of data from the three regimes will be described in detail below.

For some of the reaction conditions employed, the rate equation for the C1O time dependence did not have an analytical solution. In this case, rate coefficients were determined by obtaining the best fits between experimental absorbance data and numerical solutions of the reaction mechanism in which the rate coefficients were varied, Two separate computer codes were used to obtain the fits. One employed the conjugate gradient method and was used for very

rapid evaluation of mechanisms of limited size. The second code was the Harwell program FACSIMILE[29] which allowed symbolic input of the reaction mechanism at the expense of increased execution time.

Excess Cl_2O, *low temperature ($T \leq 250$ K).* At low temperature ("J' ≤ 250 K), the dominant channel for C1O reaction is C1OOCI formation. Under these conditions, the rate of the addition channel is at least a factor of 25 times faster than the sum of the bimolecular reaction rates. The rate of C1O dimer decomposition is also very slow; the 1/e lifetime of the dimer is greater than 20 s at T = 250 K. By neglecting the contributions from bimolecular reactions and dimer decomposition and assuming that reaction 5 is fast compared to the rate of dimer formation, the mechanism reduces to a simple second-order loss process for ClO, i.e.,

$$\frac{d[ClO]}{dt} = -k_1 [M] [ClO]^2 \qquad (10)$$

$$\frac{1}{[ClO]} = k_1 [M] t + \frac{1}{[ClO]_0} \qquad (11)$$

The results of the experiments carried out under these conditions were reported in a previous publication and will not be repeated here. Due to space limitations in the earlier paper, it was not possible to give the measured values of k_1 in tabular form, Values of k_1 at each pressure and temperature are therefore given in l'able III as WC]] as the parameters derived from fitting these data to the fall-off expression given by Troe.[28]

Excess atomic chlorine, high temperature (250 K ≤ T ≤ 400 K). A set of experiments was conducted under conditions such that photolysis of Cl_2 produced excess Cl over Cl_2O. To a first approximation, Cl remained in large excess over the time scale of the C1O + ClO reaction, The presence of excess Cl affects the reaction mechanism in three ways: first, Cl rapidly and stoichiometrically converts all of the $C1_20$ to C1O. There can therefore be no secondary regeneration of C1O by reaction 5. Second, Cl rapidly converts all of the ClOOCl produced in reaction 1 to Cl_2 and C1OO (which rapidly decomposes to Cl + 02), The net reaction is the Cl-catalyzed recombination of C1O to $C1_2$,

$$ClO + Clo \xrightarrow{M} ClOOCl \qquad (1)$$

$$Cl + ClOOCl \longrightarrow Cl_2 + Cloo \qquad (6)$$

$$ClOO \xrightarrow{M} cl + O_2 \qquad (-7)$$

Net: $C1O + C1O \longrightarrow Cl_2 + O_2$

Third, the OC1O produced in reaction 4 rapidly regenerates C1O by reaction with excess Cl (reaction -4). Reaction 4 therefore does not contribute to the loss of ClO. With the rapid removal of Cl_2O, C1OOCI and OCIO by Cl, there is no secondary regeneration of C1O on the time scale of the C1O + ClO reaction. Under these conditions, the loss of C1O in the excess Cl system is given by,

$$\frac{d[ClO]}{dt} = -(k_1[M] + k_2 + k_3)[ClO]^2 \qquad (12)$$

where ClO formation (reaction 5) is assumed to be instantaneous relative to C1O loss and transport out of the cell has been neglected. [C1O] should follow a second-order rate law with the effective rate coefficient being given by

$$k_{obs} = k_1[M] + k_2 + k_3.$$

Plots of k_{obs} vs. [M] should therefore be linear with slope k_1 and y-intercept $k_2 + k_3$.

When 02 was used as the bath gas, the time dependence of the ClO formation displayed a slower secondary increase in addition to the rapid rise due to reaction 5. This secondary formation of C1O was caused by the association reaction of chlorine atoms with oxygen to form the chlorine peroxy radical followed by reaction with atomic chlorine to form ClO, *i.e.*,

$$Cl + O_2 \xrightarrow{M} Cloo \qquad (7)$$

$$ClOO + Cl \longrightarrow 2C1O \qquad (-3")$$

The secondary ClO formation process could be readily modeled by including these reactions in the mechanism used to fit the data. Because the formation of ClO from reaction -3" was much faster than its removal by the ClO + ClO reactions, there was no impact on the uncertainty of the derived rate constants.

It was found that C1O temporal decay profiles could not be fit precisely by a second-order rate law. This was due to a partial breakdown of the excess chlorine atom assumption at long reaction times duc to direct Cl recombination (reaction 9) and ClO-catalyzed recombination (reactions 8 and 5). Under these conditions, additional terms must be included in the ClO rate equation accounting for regeneration from dimer decomposition (reaction -1) and the reaction of Cl with OC1O (reaction -4). Mechanism simulations indicate that the contribution from dirner decomposition dominates especially at high temperature and pressure (ClOOCl decomposition increases by over four orders of magnitude between T = 260 K and T = 400 K[26], while the rate of dimer formation decreases by a factor of only three.) Gas flow out of the reaction cell also made a small contribution to the C1O loss rate.

Because of these additional complications, the C1O rate equation does not have an analytical solution. Rate coefficients were determined using FACSIMILE to fit single-wavelength (275.5 nm) absorbance data from the PMT to the time-dependent absorbance change calculated by the model using the reaction mechanism in Table 1 and absorption cross sections in

l'able II. The calculated absorbance change at this wavelength is primarily due to ClO but includes minor (<10%) contributions from $ClOOCl$, Cl_2O and Cl_2. In fitting the observed absorbance curves, rate coefficients for the termolecular component (k_1), two of the bimolecular components (k_2, k_3), the Cl + ClO + M reaction (k_8) and flow through the cell (τ_{flow}) were varied while all other rate coefficients were held fixed. 'l'he rate coefficient for the Cl + OC1O product channel (k_4) was initially fixed at 2 x 10-] ^{5} cm^3 molecule^{-1} s^{-1} to reduce the number of degrees of freedom. Because OC1O is rapidly recycled, the fits were insensitive to large variations in k_4 as expected. Since k_8 controls the chlorine atom recombination and its value has not been directly measured, it was treated as a variable parameter. The final value of k_8 produced in the fits was typically within ±50% of the estimate using Troe's method. The value of τ_{flow} derived in the fitting procedure was typically ≈0. 1 s-' which compares favorably with the cell residence time of-1 5 s.

The values of k_1, k_2 and k_3 which resulted from the fitting procedure were not unique, but were dependent on the initial guess for each parameter. However, the sum of the rate coefficients for all C1O loss terms, $k_{tot} = k_1[M] + k_2 + k_3$, converged to a unique value regardless of the initial parameter guesses for these parameters. By including the effects of chlorine atom recombination and reagent flow, the computed values of $k_{tot} (= k_1[M] + k_2 + k_3)$ differed by about 15°/0 from the results using the analytic second-order rate expression, but the correction was as large as 400/0 for some runs. Figure 1 shows a typical C1O absorbance signal with the corresponding fits using the full mechanism (Figure 1a) and a second-order rate law (Figure 1 b). The visual difference between the two fits is slight with the difference best seen in the somewhat greater variation of the residuals for the fit to a second-order rate law.' The computational difference is more apparent--the sum of the squared' residuals is 35% greater for the second-order rate law fit compared to the full mechanism fit.

As indicated in the preceding discussion, plots of k_{tot} vs. [M] should be linear with the slope and y-intercept corresponding to k_1 and $k_2 + k_3$, respective y. An example of such a plot is given in Figure 2 for M = N_2. While all the data plots are linear, a dependence of the intercept on $[Cl_2]$ is observed. Because $C1_2$ photolysis was used as the chlorine atom source and the fractional dissociation of Cl_2 is low (-0.2%), high Cl_2 concentrations (5 -18 x 10^{16} molecule cm^{-3}) were necessary to produce a large excess of chlorine atoms. A likely explanation for the $[Cl_2]$ dependence is the varying contribution of $C1_2$ to the overall collisional efficiency of the bath gas. The effective reaction is

$$ClO + ClO + Cl_2 \longrightarrow ClOOCl + Cl_2 \qquad (1')$$

although the energy transfer from vibrational 1 y excited ClOOCl is probably catalyzed by a stable complex, as discussed below. With the third body effect of Cl_2 included, the expression for k_{tot} is given by

$$k_{tot} = k_1 [M] + k_2 + k_3 + k_1'[Cl_2]$$

where k_1' is the termolecular rate coefficient with M = Cl_2. Because reactions 1 and 1' both produce ClOOCl, the fitting routine cannot differentiate between the two processes and lumps all the dimer formation processes into reaction 1. The individual rate coefficients can be extracted from k_{tot} by first plotting k_{tot} vs. [M] which has a slope of k_1 and a y-intercept of $k_2 + k_3 + k_1'[Cl_2]$. A plot of this y-intercept vs. $[Cl_2]$ will have a slope of k_1' and a y-intercept of $k_2 + k_3$.

C1O loss data were collected at temperatures ranging from 260-390 K, pressures ranging from 50-700 Torr and $[Cl_2]$ ranging from 5-18 x 1016 molecule cm^{-3}. A plot of k_{tot} vs. $[N_2]$ for a number of $C1_2$ concentrations at T = 350 K is shown in Figure 2, and a plot of the resulting y-intercepts vs. $[Cl_2]$ is shown in Figure 3. The calculated value of k_1 at a given temperature was obtained by averaging the slopes for all plots of k_{tot} vs. $[N_2]$ such as Figure 2. An Arrhenius plot of k_{1,N_2} over the range T = 195-390 K is shown in Figure 4a in which dimer formation rate coefficients from both low temperature/excess $C1_20$ and high temperature/excess Cl experiments arc included. The temperature dependence expressed in Arrhenius form is $k_{1,N_2}(T) = (1.221$ O. Is).x 10^{-33} $\exp\{(833 \pm 34)/T\}$ cm^6 $molecule^{-2}$ s^{-1}. An alternate expression for the temperature dependence, in which the data is plotted in log-log form shown in Figure 4b, is $k_{1,N_2}(T) = (2.07 \pm 0.09) \times 10^{-32} \{T/300\}^{-(3.01 \pm 0.20)}$ cm^6 $molecule^{-2}$ s^{-1}. Dimer formation rate coefficients with N_2 as a third body are summarized in Table IV. Table V summarizes the y-intercepts of the plots of k_{tot} vs. $[N_2]$ as a function of $[Cl_2]$. Figure 5 shows the sum of the bimolecular rate coefficients, $k_2 + k_3$, in Arrhenius form. The sum is expressed as $(k_2 + k_3)(T) = (1.78 \pm O.19) \times 10^{-11} \exp\{-(2150 \pm 450)/T\}$ cm^3 $molecule^{-1}$ s^{-1}.

The efficiency of dimer formation as a function of bath gas was studied at 300 K. Plots of k_{tot} vs. [M] for M = He, Ar, N_2, 0_2, CF_4 and SF_6 are shown in Figure 6. As discussed above, the slopes of each plot give $k_{1,M}$. The values of $k_{1,Cl_2}(T)$ were determined from the slopes of the plot of $k_2 + k_3 + k_1'[Cl_2]$ vs. $[Cl_2]$ (see Figure 3) at each temperature. The results for each bath gas at 300 K as well as the variation of k_{1,Cl_2} as a function of temperature are summarized in ~'able VI.

Excess Cl_2O, high temperature(250 $K \leq T \leq$ 400 K). A series of experiments was conducted over the temperature range 250-400 K using excess Cl_2O over Cl. In these experiments, both C1O and OC1O were monitored. As with the excess $C1_20$ experiments at temperatures below 250 K, the chlorine atoms initially formed from Cl_2 photolysis are rapidly converted to C1O. Above 250 K, the C1O + C1O bimolecular channels contribute to the formation and removal of C1O. Reaction 3 produces two Cl atoms; one from the direct bimolecular

reaction and another from the rapid thermal decomposition of C1OO (reaction -7). These Cl atoms will be quickly titrated by Cl_2O (reaction 5) to regenerate C1O. The overall result of reaction 3 is no net loss of ClO. Similarly, the Cl atom produced in reaction 4 regenerates one C1O molecule. The effect of Cl + ClOOCl (reaction 6) on the C1O kinetics is also negligible. Even though the rate coefficient of reaction 6 is comparable to the titration step (reaction 5), kinetic simulations using the full reaction mechanism indicate that the maximum concentration of ClOOCl produced is approximately 200 times less than the $C1_20$ concentration, and thus ClOOCl cannot compete with Cl_2O for the removal of Cl. Thus, neglecting the effect of C1OOCI decomposition, the observed second-order rate coefficient for C1O loss from the bimolecular channels is given by

$$k_{obs} = k_2 + \tfrac{1}{2}k_4.$$

The time dependence of the OClO product also provides kinetic information. Neglecting C1OOC1 decomposition, the OClO time dependence is given by

$$[OClO] = [ClO]_o \frac{\frac{k_4}{2}}{2\left(k_2 + \frac{k_4}{2}\right)} \left\{ \frac{2[ClO]_o\left(k_2 + \frac{k_4}{2}\right)t}{2[ClO]_o\left(k_2 + \frac{k_4}{2}\right)t + 1} \right\}$$

Under these conditions, a plot of $1/[OClO]$ vs. $1/t$ has a slope of $(\tfrac{1}{2}k_4[ClO]_o^2)^{-1}$ and an intercept of $2(k_2+\tfrac{1}{2}k_4)/(\tfrac{1}{2}k_4[ClO]_o)$. By monitoring OC1O, k_2 and k_4 can therefore be determined individually, and the values of $k_2 + \tfrac{1}{2}k_4$ derived separately from the ClO and OC1O data can be checked for consistency.

A significant complication is posed by the effect of ClOOCl decomposition. Above 250 K, C1OOCI decomposition cannot be neglected and at temperatures above 300 K, C1OOC1 approaches equilibrium with CIO on a time scale comparable to the loss of C1O by the bimolecular channels. The resulting rate equation for C1O is

$$\frac{d[ClO]}{dt} = -(k_1[M] + k_2 + \frac{1}{2}k_4)[ClO]^2 + 2k_{-1}[M][Cl_2O_2] \qquad (13)$$

Since this equation does not have an analytical solution, FACSIMILE was used to analyze both the CIO and OC1O kinetic data. The mechanism for conditions of excess Cl_2O consisted of reactions 1, -1, 2, 4, 5 and flow through the cell. The use of this relatively small subset of the reactions in Table I was possible because the combination of the large excess of $C1_20$ and the large rate coefficient for reaction 5 precluded the scavenging of Cl by any species other than $C1_20$, a fact that was verified using simulations. Initially, the objective was to determine the rate coefficients for the bimolecular reactions, k_2 and k_4. The procedure that was employed was to fix the rate coefficients that determined the 2C1O-C1OOC1 equilibrium (k_1 and k_{-1}). The mechanism used values of k_1 determined in the excess Cl experiments and, as a starting point, values of k_{-1}

were used as inferred from the equi Ii brium constant measurements of Cox and Hayman.[20] In the fitting procedure, the values of k_2, k_4 and τ_{flow} were varied.

Another complication in the data analysis for the excess $C1_20$ experiments above 250 K arises due to changes in the absorption baseline (l.) caused by removal of $C1_20$ during the reaction. Both reactions 3 and 4 produce Cl which catalyze the removal of Cl_2O. Although reaction 3 is a propagation step and does not result in the loss of ClO, the effect on the baseline change is non-negligible since the chain length for Cl_2O removal is about 6. The changing baseline introduces an ambiguity in the measurement of C1O in the PMT experiments in which ClO is monitored at a single wavelength. In attempting to fit the single wavelength data without reaction 5, the routine became non-deterministic because there is insufficient information to fit the decay curves without prior knowledge of the Cl_2O removal rate. in the excess Cl_2O experiments below 250 K, the effect of the baseline shift due to changes in Cl_2O is negligible because reactions 3 and 4 become very slow, however, a small analytic correction due to residual absorption of C1OOCI was required, as discussed above.

The remedy for this problem was the use of an OMA for data acquisition in which a portion of the absorption spectrum of either ClO or OClO was collected as a function of time. The time-dependent spectra were compared to a reference spectrum of known concentration to determine directly the concentrations of each species. Because this is a differential absorption technique, the artifact associated with the baseline change is eliminated. An example of an OClO signal and the associated fit are shown in Figure 7. The inset of Figure 7 displays a typical OC1O spectrum from a single scan of the OMA fit to the reference spectrum. Because of the multiplex advantage of the OMA and the resulting high signal-to-noise-ratio, it was possible to obtain fits for k_2 and k_4 with very good precision. The temperature dependent rate coefficients are displayed in Arrhenius form in Figure 5, and the data arc summarized in Table VII. The rate coefficient expressions for each bimolecular channel are $k_2(T) = (1.01 \pm 0.12) \times 10^{-12} \exp\{-(1590 \pm 100)/T\}$ cm^3 $molecule^{-1}$ s^{-1} and $k_4(T) = (3.50 \pm 0.31) \times 10^{-11} \exp\{-(1370 \pm 150)/T\}$ cm^3 $molecule^{-1}$ S-l. With k_2 determined under conditions of excess $C1_20$, and $k_2 + k_3$ determined under conditions of excess Cl, the rate coefficient expression for k_3 was calculated from the difference between these expressions. This resulted in $k_3(T) = (2.98 \pm 0.68) \times 10^{-11} \exp\{-(2450 \pm 330)/T\}$ cm^3 $molecule^{-1}$ S-l.

C1O removal also was monitored using the OMA at 340 K and 370 K in order to check the consistency of the bimolecular rate coefficients determined by monitoring C1O with those measured above while monitoring OClO formation. The reaction mechanism consisted of reactions 1, -1, 2, 5 and flow with k_2 and τ_{flow} as varied parameters and k_1, k_{-1} and k_5 held fixed. In this case, the value of k_2 derived in the fitting routine is actually a measure of the total rate of C1O termination by the bimolecular channels and is equivalent to $k_2 + \frac{1}{2}k_4$. Reaction 4 was

excluded because the C1O data provide no direct information on the OClO yield. A typical ClO signal and the corresponding fit are shown in Figure 8 with the inset illustrating a fit of the C1O reference spectrum to the. OMA data. The values derived for $k_2 + ½k_4$ are given in the last column of Table VII. For comparison, values of $k_2 + ½k_4$ from the OClO data arc also shown. The agreement is better than 10%.

The activation energy of the OC1O + Cl channel determined in this study is $E_a = 2.72 \pm 0.30$ kcal mol^{-1}. This value, combined with the activation energy of the reverse reaction[26] (E_a = -0.32 kcal me]$^{-1}$), gives an enthalpy of reaction 4 of $\Delta H^o = 3.04$ kcal mol^{-1}. The enthalpy of formation of OClO calculated from this result is $\Delta H^o_{f,OClO}(298) = 22.6 \pm 0.3$ kcal mol^{-1} which compares favorably with the most recent value reported in the JANAF tables[30] of $\Delta H^o_{f,OClO}(298) = 23.2 \pm 1.9$ kcal mol^{-1}. In addition, the value of $AH^0_{foc10}(298)$ derived from this work has a significantly smaller uncertainty.

The experiments carried out above 250 K with excess Cl_2O provided a means to determine rate coefficients for the unimolecular decomposition of ClOOCl. Above 250 K, it was possible to choose a diluent gas pressure above which the time scale for the equilibrium

$$2ClO \xleftrightarrow{M} ClOOCl$$

was much faster than the time scale for C1O termination by the bimolecular channels. The ClO decay in Figure 8 illustrates this separation of time scales for an experiment carried out at a temperature of 300 K and a total pressure of 200 Torr of N_2. The initial steep drop in ClO concentration is due to the establishment of the equilibrium between C1O and C1OOC1, and the subsequent slow decay is due to bimolecular termination. The temporal regimes for these processes are clearly separable. This is also important in the determination of the rate coefficients for reactions 1-4 described above, The fitting routines for each stoichiometric case were quite insensitive to the precise value of k_{-1}, so errors in this parameter had no significant effect on the derived rate coefficient expressions for k_1, k_2, k_3 and k_4. The temperature dependent expression for k_{-1} inferred from the data of Cox and Hayman[20] was used in these mechanisms.

By using the measured values of k_1, k_2 and k_4, improved values of k_{-1} could be determined by monitoring the loss of C1O, under conditions of low temperature and pressure where the contribution from the bimolecular channels is small and the establishment of equilibrium between C1O and C1OOC1 occurs on a time scale consistent with the data acquisition time, The C1O signal was monitored with the OMA over a temperature range of 260-310 K and a pressure range of 25-300 Torr. Signals were fit to a simplified mechanism which consisted of reactions 1, -1, 2, 5 and flow through the cell. The value of k_1 was determined from the rate coefficient expression reported in this paper. As previously mentioned when monitoring ClO

loss under conditions of excess $C1_20$, k_2 represents the sum of reaction 2 and one half of reaction 4, so the value used in the fits was given by $k_2 + ½k_4$. $k._1$ was the only parameter varied in the fitting routine with the results given in Table VIII.

The C1O-C1OOC1 equilibrium constant as a function of temperature was calculated from the measured values of k_1 and k_{-1}. Values of $K_P(T)$ are summarized in Table VIII, and a van't Hoff plot of $\ln[K_P]$ vs. T^{-1} is shown in Figure 9. The enthalpy of reaction 1 calculated from the slope of the van't Hoff plot is $AH^O = -19.5 \pm 0.7$ kcal mol^{-1}, and the entropy change derived from the y-intercept is $AS^O = -41.4 \pm 2.4$ cal mol^{-1} K^1. This 2nd Law analysis resulted in a heat of formation of C1OOCI of $\Delta H^o_{f,ClOOCl}(298) = 28.9 * 0.7$ kcal mol^{-1} and $S^o_{ClOOCl} = 67.2 \pm 2.4$ cal mol^{-1} K^{-1}.

The thermochemistry of the ClOOCl intermediate may also be determined from the 3rd Law. Using standard statistical mechanical formulas, the entropy of C1OOC1 was calculated using vibrational frequencies of 752.6, 649.9, 560, 440, 320 and 127 cm^{-1}, and rotational moments of inertia of $I_A = 6.4209415 \times 10^{-39}$ g cm^2, $I_B = 35.306628 \times 10$-39 g cm^2 and $I_C = 39.722506 \times 10$-39 g cm^2. The values of 752.6 and 649.9 cm^{-1} were determined from matrix isolated IR spectra; 3. these features correspond well to features observed by Burkholder *et al.*[23] at 753 and 653 cm-' who also observed a feature at 560 cm^{-1}. The transition at 127 cm^{-1} was estimated from the microwave spectrum.[32] The transitions at 440 and 320 cm^{-1} were taken from the calculations of Rendell and Lee.[33] Variation of these values by uncertainties consistent with the discrepancies within the literature has a maximum effect of -1.0 cal mol^{-1} K^{-1} on the calculated ClOOCl entropy. Rotational constants used were those of Birk *et al.*[31] This calculation yielded $S^O_{cloocl} = 72.2 \pm 1.0$ cal mol^{-1} K^{-1}. The average enthalpy of reaction 1 calculated by this method was $AH^O = -18.1 \pm 0.2$ kcal mol^{-1}, resulting in a ClOOCl heat of formation of $\Delta H^o_{f,ClOOCl}(298) = 30.5 \pm 0.2$ kcal rnol^{-1}. The expression for the equilibrium constant obtained using this method is $K_{eq}(T) = (1.24 \pm 0.18) \times 10$-27 exp{(8820 ± 440)/T} cm^3 molecule-1 This compares to the current NASA evaluation of $K_{eq}(T) = 3.0 \times 10$-27 exp{(8450 ± 850)/T) cm^3 molecule^{-1}.[26] Using equilibrium constant values computed from the above equation, the temperature dependence for k_{-1} consistent with the 3rd Law anal ysis and the rate of dimer formation is given by, $k_{-1}(T) = (9.81 \pm 1.32) \times 10$-7 exp{-(7980 ± 320)/'1'} cm^3 molecule^{-1} s-?

The difference between the C1OOC1 entropies calculated from statistical mechanics and the 2nd Law analysis (5.0 cal mol^{-1} K-]) is not unusually large[34] but cannot be resolved by invoking the maximum error bounds of all parameters used in each determination. In the 3rd Law analysis, the vibrational frequencies of ClOOCl are the most uncertain input parameters, but the vibrational contribution to the total entropy is small compared to the translational and rotational contributions, and so varying the frequencies by the maximum possible errors has littl c

effect on the calculated entropy. Similarly, the experimental data used in the van't 1 loff plot of Figure 9 is sufficiently precise that the error bound on the y-intercept is only ±2.4 entropy units. Since the entropy of C1OOC1 is constrained reasonably well by the available spectroscopic data and the entropy change obtained from the van't Hoff equation involves a long extrapolation, the enthalpy change derived from the 3rd Law analysis is considered to be the preferred method.

Discussion

Uncertainties and sensitivities. The methods used to abstract rate coefficient information from the actual experimental data involved a number of assumptions about the relative importance of the elementary reactions in the mechanism outlined in Table I and a significant amount of numerical manipulation of the raw data, In order to have confidence in the derived rate coefficient expressions, it is necessary to understand the sensitivity of the calculated rate coefficient values to these assumptions and the uncertainties introduced by the numerical analysis procedure.

Under conditions of excess atomic chlorine, the mechanism employed in the fitting routine was comprised of 15 elementary reactions. The value derived from the data under these conditions was the total rate of C1O loss given by $k_{tot} = k_1[M] + k_2 + k_3$. Figure 10 illustrates the effect of uncertainties in the rate coefficients held fixed in the fitting procedure on k_{tot}, and the sensitivity of the mechanism to variations in those rate coefficients. The percent change in the calculated value of k_{tot} was determined by performing fits of the data to the reaction mechanism, as was done in the preceding section to determine k_{1,N_2} and $k_2 + k_3$, where the input value of each rate coefficient held fixed in the procedure was individually varied by its reported uncertainty. Figure 10 indicates the magnitude of the possible errors introduced into the calculated k_{tot} from the uncertainty of the rate coefficients used in the fitting procedure, As can be seen, the uncertainties of the known rate coefficients have little effect on the derived value of k_{tot}, the greatest change being only -0.6°/0 of the fitted value of k_{tot}. For example, the reported value of k_{-7} has an uncertainty factor of 3, yet varying the value of k_{-7} in the fitting routine by +-/- this uncertainty produces a change in k_{tot} of only -0.4% and -0.6%, respectively. Thus, the mechanism used in determining k_{tot} is quite insensitive to the exact value of k_{-7}. The same is true of all the rate coefficients. Uncertainty factors for each rate coefficient arc included in parentheses in Figure 10. The overall effect of uncertainties in the input parameters for the fitting procedure on the determination of k_{tot} is very small so that the error bounds reported for k_1 and k_3 are an indication of the precision of the data, and are not introduced by the process of fitting the data to the reaction mechanism.

Examination of Figures 3 and 4 gives an indication of the source of scatter in the analysis procedure, particularly for the bimolecular rate coefficients measured under excess Cl conditions.

The process required to abstract individual rate coefficients from k_{tot} involved fitting the data up to three times with each successive fit being dependent on the previous results. The values derived for $k_2 + k_3$ and k_{1,Cl_2} are dependent on the y-intercepts of plots such as Figure 2. Uncertainties associated with the y-intercept of plots of k_{tot} vs. $[N_2]$ will be propagated through to the values derived from plots of the y-intercept vs. $[Cl_2]$. Additionally, it was not possible to reduce the concentration of Cl_2 to values near zero and still maintain an excess of Cl atoms over Cl_2O, thus making it necessary to extrapolate over a fairly wide region with no data points in order to obtain the value of $k_2 + k_3$ in plots of the y-intercept vs. $[Cl_2]$. The uncertainties associated with these assumptions are reflected in the large error bounds for $k_2 + k_3$ in Figure 5. The resulting rate coefficient expressions arc $k_{1,N_2}(T) = (1.22 \pm 0,15) \times 10\text{-}33 \exp\{(833 \pm 34)/T\}$ cm^6 $molecule^{-2}$ $s^{-}]$ or, alternately, $k_{1,N_2}(T) = (2.07 \pm ().()9) \times 10^{-32}\{T/300\}^{-3.01 \pm 0.20}$ cm^6 $molecule^{-2}$ s^{-1} and $k_3(T) = (2.98 \pm 0.68) \times 10^{-11} \exp\{-(2450 \pm 450)/T\}$ cm^3 $molecule^{-1}$ s-' where the error bounds are an indication of the precision of least-squares fits to the respective Arrhenius plots.

A similar analysis of the data under conditions of excess Cl_2O is shown in Figure 11 for the determination of k_2 and k_4. In this case, the dimensionality of the mechanism was reduced to six elementary reaction. As in the excess chlorine atom case, uncertainties in the rates of the titration reaction (k_5) and flow through the ccl] were not considered. The error bounds used for the rate coefficient of dimer formation were determined from the least-squares fits of Figure 4a. The uncertainties in k_2 and k_4 introduced by the data fitting procedure are greater than those of k_{tot} determined under *excess* chlorine atom conditions with maximum deviation from the fitted values of 110/0 for k_2 and 9°/0 for k_4, 1 lowever, these values are less than the uncertainties derived from a least-squares fit of the Arrhenius plots. Because the values of k_2 and k_4 were determined directly from the FACSIMILE fitting routine, the uncertainties in these parameters are much smaller than those of k_3. This is evident in the respective plots of Figure 5. The error bounds derived from the precision of the least-squares fits are ±1 8'% for k_2 and ±30% for k_4. ~'bus, the largest uncertainty in the values of k_2 and k_4 arises from the statistics of the Arrhenius plots and not from the kinetics anal ysis procedure of fitting the data to the reaction mechanism. The error bounds are given by $k_2(T) = (1.01 \pm 0.12) \times 10^{-12} \exp\{-(1590 \pm 100)/T\}$ cm^3 $molecule^{-1}s^{-1}$ and $k_4(T) = (3.50 \pm 0.31) \times 10^{-13} \exp\{-(1370 \pm 150)/T\}$ cm^3 molecule-l s^{-1} where the error bounds are a measure of the precision only.

For the determination of the rate coefficient of C1OOCI thermal decomposition, the errors introduced in the fitted value of k_{-1} are shown in Figure 12 for the two parameters used as input in the fitting routine. Error bounds for k_1 and $k_2 + \frac{1}{2}k_4$ were those determined in the above analysis. The resulting uncertainty in k_{-1} is 14% from k_1 and 12% from $k_2 + \frac{1}{2}k_4$. This is approximate] y equal to the uncertainty determined from the precision of a plot of $\ln[k_{-1}]$ vs. $1/T$.

The error bounds are expressed as $k_1(T) = (1.26 \pm 0.17) \times 10^{-5} \exp\{-(8700 \pm 340)/T\}$ cm^3 $molecule^{-1}s^{-1}$.

C1O *association rate constant (low-pressure limit).* The temperature dependence of the rate constant for ClO association (reaction 1) in the low-pressure limit has been measured previously over limited temperature ranges. I layman *et al.]* [7] reported a value of $k_{1,N_2}(T) = (6.0 \pm 0.37) \times 10^{-32} \{T/300\}^{-2.1 \pm 0.7}$ cm^6 $molecule^{-2}s^{-1}$ measured over the range 1' =- 268-338 K. Trolier *et al.*[8] reported a value of $k_{1,N_2}(T) = (1.34 \pm 0.09) \times 10^{-32} \{T/300\}^{-3.9 \pm 0.3}$ cm^6 $molecule^{-2}s^{-1}$ measured over the range T = 200-263 K. Sander *et al.*,[7] *whose* data arc included as the low temperature results reported in this study, derived the expression $k_{1,N_2}(T) = (1.8 \pm 0.5) \times 10^{-32} \{T/300\}^{-3.6 \pm 1.0}$ cm^6 $molecule^{-2}s^{-1}$ based on the data taken over the temperature range 195 -247 K. The C1O association rate coefficient measured in the present experiments is in relatively good agreement with these values, although the temperature dependence is not as strong as that reported by Trolier *et al.* and Sander *et al.* The temperature over which measurements were taken for each of these previous studies was limited to a range of approximately 60 K. In the present results, which include the data published by Sander *et al.,* the temperature regime ranged from 195 to 390 K and encompassed the individual ranges covered by all of the previous studies. The values of $k_{1,N_2}(T)$, shown in Figure 4a, display good linearity over the entire temperature range when plotted in Arrhenius form. However, when plotted as $\ln[k_1]$ vs. $\ln[T/300]$, as was done in the previous studies, shown in Figure 4b, the data exhibit a systematic departure from linearity. This is most apparent at the temperature extremes of Figure 4b. The data at the lowest and highest temperatures lie above the fitted line, and the data at mid temperatures lie below the fitted line. This is in contrast to the Arrhenius plot of Figure 4a in which the scatter of the data points about the fitted line is more random. The data of Figure 4b would best be fit by a curve with a slope that decreases as temperature increases. This is an indication that a log-log analysis does not describe the data as accurately as the Arrhenius form. This explains the stronger temperature dependence seen earlier--when only the data at low temperature are analyzed using a log-log form, the apparent slope of' the plot is steeper than would be seen for experiments which extend over a wider temperature range.

Because of the relatively large temperature dependence of k_1 in the low-pressure limit, falloff behavior for reaction 1 is observable only at temperatures below about 250 K. Sander *et al.* [7] obtained a high-pressure limiting rate constant of $k_{1,\infty}(T) = (6 \pm 2) \times 10\text{-}12\ (T/300)^{0 \pm 1}$ cm^3 molecule-l s^{-1} when fitting the falloff data with a broadening factor (F_c) of 0.6 (see Table 111). Trolier *et al.*[8] obtained a value of (4.8 ± 0.5) x 10-12 $cm^3 molecule^{-1}s^{-1}$ (independent of temperature) for $k_{1,\infty}$ when their data were fit neglecting the bimolecular intercept.

The dependence of k_1 on bath gas (see Figure 6 and 'l'able VI) follows the expected trend for third body quenching efficiency with the exception of 0_2 and $C1_2$. Previous studies of the

chlorine-photosensitized decomposition of O_3 have reported that 0_2 reduces the quantum yield for O_3 destruction, Φ_{O_3}, relative to the same experiments carried out in N2. in the studies of Lin *et* al.,[19] the T = 298 K, Φ_{O_3} was 6 in N2 while a value of 4 was obtained in 0_2. At 1' = 240 K, the results were identical for both bath gases. Since the quantum yield should depend only on the branching ratios of the bimolecular channels, the bath gas should have no effect, To explain this bath gas effect, it has been postulated that the products formed in the bimolecular channels arc not the result of "direct" reactions, but rather that all reaction channels proceed through one or more $(ClO)_2$ isomers and subsequently undergo unimolecular decomposition to produce the specified set of products. That $k_{1,0_2}(300)$ measured in this study is 38% slower than $k_{1,N_2}(300)$ and 27% slower than $k_{1,Ar}(300)$ may bc an indication that 0_2 is more actively involved in the chemistry of the $(C10)_2$ intermediate than simply playing the role of a third body energy quencher. Trolier et *al.*[8] measured a k_{1,O_2}:k_{1,N_2} ratio of 0.82, and Sander *et al.*[7] measured a ratio of 0.94 compared to the present result of k_{1,O_2}:k_{1,N_2} = 0.62. The two previous studies were conducted over temperature ranges much colder than 300 K where dimer formation dominates, and the bimolecular channels are negligible, and hence may not reflect the possible effect of 0_2 on the bimolecular channels present in the current room temperature experiments.

The rate coefficient for dimcr formation with Cl_2 as a third body is greatly enhanced relative to the value expected from vibrational energy transfer arguments. The value of k_{1,Cl_2} at 300 K is more than three times greater than k_{1,N_2}, and is more than twice as large as k_{1,SF_6} which is considered to be a very efficient vibrational energy quencher. $k_{1,Cl_2}(T)$ also displays a unique temperature dependence with the rate coefficient reaching a minimum at 300 - 310 K and increasing dramatically at both lower and higher temperatures. "l'he low temperature behavior of k_{1,Cl_2} may bc explained by invoking a chaperone mechanism in which a C10-$C1_2$ intermediate is formed which facilitates subsequent reaction with ClO, *i.e.*

$$ClO + Cl_2 \longrightarrow ClO\text{-}Cl_2 \qquad (15)$$

$$C1O\text{-}CI2 + ClO \longrightarrow ClOOCl + Cl_2 \qquad (16)$$

Indeed, recent quantum chemical calculations suggest the existence of a weakly bound C10-$C1_2$ species.[35] The rapid rise of k_{1,Cl_2} at higher temperature cannot be explained at this time. Whether this increase is due to an unknown bimolecular reaction between C1O and Cl_2 or the formation of some stable intermediate is not currently understood.

The presence of an enhanced C1O recombination rate in the presence of $C1_2$ may help to explain an anomaly observed by Trolier *et al.*[8] Trolier *et al.* obtained better fits to their falloff plots by including a temperature-dependent intercept in the zero-pressure limit. This intercept varied from 6.7 (+7.6/-4.0) x 10-14 cm^3 molecule-l s^{-1} at 200 K to 2.7 (+ 1.0/-0.9) x 10^{-14} cm^3 molecule^{-1} s^{-1} at 298 K. They speculated that the intercept might be due to a pressure

independent decomposition pathway of vibrationally excited ClOOCl (forming $Cl_2 + 0_2$) or to the influence of multiple potential energy surfaces forming C1OOC1. The results from the present study indicate that the first suggestion is unlikely since all the product pathways resulting from decomposition of vibrationally excited ClOOCl proceed over barriers which make the net reactions very slow at 200 K.

There is another explanation, however, for the intercepts observed by Trolier *et al.* In their study, Cl_2 concentrations around 6 x 1016 molecule cm^{-3} were employed, A measurement of k_1 for M = Cl_2 was made at 200 K by Trolier et *al.* and found to be about 1.1x10-3] cm^6 $molecule^{-2}$ s^{-1} from measurements over a limited range of [Cl_2]. This value was used to correct all their kinetic data, presumably at all temperatures. In contrast, extrapolation of the low temperature k_{1,Cl_2} from this study (see 3'able VI) to 200 K gives a value of (7.0 ± 3.5) x 10-3' cm^6 $molecule^{-2}$ s^{-1} Using this rate constant and the Cl_2 concentrations used by Trolier *et al.*, there should have been a pressure-independent contribution to the apparent ClO + ClO + M association rate constant of about 4 x 10^{-14} cm^3 $molecule^{-1}$ s^{-1} at 200 K. "l'his is in good agreement with their observed value, and implies that Trolier *et al.* undercorrected for the enhanced third-bod y effect of $C1_2$, and that this effect accounts for their observed intercept. 1 n the present study (falloff data reported in ref. 7), Cl_2 concentrations were about an order of magnitude smaller which would lead to a negligible intercept in the low temperature data.

ClOOCl thermal decomposition. '1'here arc no previous direct determinations of the rate coefficients for ClOOCl thermal decomposition. The best comparison with previous work is between the equilibrium constants calculated from our measurements of k_1 and k_{-1}, and the equilibrium constant measurements of Cox and I layman.[20] As shown in Figure 9, over the temperature range of the present experiments (260 K ≤ T ≤ 310 K) the data sets arc very consistent. However, Cox and Hay man include several data points in their van't Hoff plot with large error bounds at lower temperatures which do not fall precisely on the trend line suggested by the higher temperature data. As a result, the slope of the line derived from the least-squares fit to all of the Cox and Hayman data is significantly smaller than that derived from the data in this study. The thermodynamic data derived from this work (Al $I^o_{f,ClOOCl}(298)$ = 30.5 ± 0.7 kcal me]-], and S^o_{cloocl} = 72.2 ± 1.0 cal mol^{-1} K^{-1}) differ from the values obtained from Cox and Hayman's 2nd Law analysis ($\Delta H^o_{f,ClOOCl}(298)$ = 31.3 ± 0.7 kcal mol^{-1}, and S^o_{cloocl} = 73.2 ± 2.6 cal $mol^{-1}K^{-1}$) and result in a stronger calculated 0-0 bond energy for ClOOCl (18.1 kcal mol^{-1} from this study vs. 17.3 kcal mol^{-1} measured previousl y),

Analysis of the dimer decomposition data and calculation of equilibrium constants was done assuming that the only form of the dimer produced in the C1O association process was chlorine peroxide, C1OOC1. This assumption was based on the results of Birk *et al.* [32] who quantified the yield of ClOOCl from the C1O + ClO reaction using submillimeter absorption

spectroscopy. l-his conclusion is also reinforced by recent *ah initio* calculations. Using the CCSD(T) method with a large basis set, Lee *et al.*[36] calculate that the asymmetric dimer, C1OClO, lies (10.1 ± 4.0) kcal mol^{-1} above ClOOCl. Because the binding energy of the asymmetric dimer is considerably less than that of chlorine peroxide, it is not likely that ClOClO will produce a measurable contribution in the ClO kinetics. To verify this assumption, simulations of the time-dcpcndcnt ClO concentration, including and excluding ClOClO formation, were performed using the ClO + C1O rate coefficients measured in this study. The rate coefficient for C1OC1O formation was set equal to the rate coefficient for ClOOCl formation, and the C1OC1O dissociation rate was calculated assuming the same A-factor as ClOOCl dissociation with an activation energy 10 kcal mo]$^{-1}$ less than for C1OOCI. The result was no perceptible diffcrcncc in ClO concentrations. "l'his would suggest that the asymmetric dimer is unimportant. However, it is necessary to proceed through an asymmetric transition state in order to form the OClO product of reaction 4. Whether the asymmetric transition state is formed by a direct process from ClO association or by isomerization of chlorine peroxide cannot bc determined from our data.

Bimolecular channels. Activation energies dctcrmincd from the individual rate coefficient expression for each bimolecular channel arc $E_{a,Cl_2+O_2} = 3.16 \pm 0.20$ kcal mol^{-1}, $E_{a,ClOO+Cl} = 4.87 \pm 0.89$ kcal me]$^{-1}$ and $E_{a,OClO+Cl} = -2.72 \pm 0.30$ kcal mol^{-1}. The ClO + ClO energy diagram is shown in Figure 13 with all relevant intermediate and product channel energies. The heat of formation of OClO was calculated from the activation energies of the forward and reverse of reaction 4. This gave $\Delta H^{o}_{f,OClO}(298) = 22.6 \pm 0.3$ kcal mol^{-1} which is in excellent agreement with the current value from the JANAF Table[30] of $\Delta H^{o}_{f,OClO}(298) = 23.2 \pm 1.9$ kcal mol^{-1}.

The observed activation energy for the formation of ClOO + Cl ($E_a = 4.87$ kcal mol^{-1}) is the highest of the three bimolecular channels. The reverse reaction has two exothermic channels:

$$ClOO + Cl \longrightarrow Cl_2 + O_2 \qquad (-3')$$

$$\longrightarrow ClO + ClO \qquad (-3'')$$

Although reaction -3 has been studied by a number of investigators,[26] channel-specific Arrhenius parameters are not available. At room temperature, $k_{-3'}/k_{-3''}$ is about 20, and the overall rate constant is independent of temperature. From the currently tabulated enthalpies of formation of Cl, ClO and C1OO and the activation energy for reaction 3 determined in this work, the activation energy for reaction -3" is predicted to be about (1.8 ± 1.5) kcal mole* (see Figure 13). This leads to a value for the ratio $k_{-3'}/k_{-3''}$ of 20 (with an uncertainty of a factor of 10), assuming that reaction -3' is temperature independent and that the A-factors for reactions -3' and -3" arc equal. This is in excellent agreement with the observed branching ratio. The large uncertainty is

due primarily to the uncertainty in the enthalpy of formation of ClOO (± 1 kcal mole-1). The assumption of nearly equal A-factors for reactions -3' and -3" is justified by 1) calculations of the relative entropies of activation for the two channels using the known ClOOCl geometry and an estimated structure for ClClOO based on matrix studies of C1C10[37-39] and 2) analogy with the reaction

$$Cl + HO_2 \longrightarrow HCl + O_2$$

$$\longrightarrow OH + ClO$$

for which the measured A-factors arc within a factor of 2.[26] Direct studies of the temperature dependence of reaction -3" would be useful in this regard.

Past experimental studies of the overall rate constant for the bimolecular channels and the branching ratios have suffered from a number of complications including secondary reactions which regenerate C1O via channels 3 and 4, and formation and decomposition of C1OOC1 on the time scale of the experiment. In addition, most experimental systems have relied upon ultraviolet absorption for the detection and measurement of ClO, OC1O, C1OO and Cl_2 in these experiments. Because the time dependence of [ClO] is governed by a second-order or more complex rate law, the absolute concentration of ClO radicals must be determined. Problems associated with the measurement of ClO cross sections, as well as the presence of interfering absorbers have therefore provided additional complications. As a result, the overall rate constant and branching ratios for the bimolecular channels have remained poorly established.

The results of previous studies of the bimolecular channels of reaction 1 have been summarized by Simon *et al.*[18] Measured values for the overall rate constant for the bimolecular channels at 298 K, $k_2 + k_3 + k_4$, range between 0.57 and 11.3 x 10-'4 cm^3 molecule-l s^{-1} with values of 1.2 and 1.0 x 10-14 cm^3 $molecule^{-1}s^{-1}$ being recommended by the NASA and IUPAC data evaluation panels, respectively (DeMore *et* al.,[26] Atkinson *et al.*[42]). The temperature dependence of the overall reaction was measured by Porter and Wright[3] who found the overall rate constant to bc independent of temperature over the range 293-433 K, and Clyne and Coxon[10] who obtained the expression, $k_{obs} = (5.8 \pm 1.7) \times 10^{-13} \exp\{-1250/T\}$ cm^3 $molecule^{-1}$ s^{-1} over the temperature range 300-450 K.

Branching ratios for the bimolecular components of the ClO + ClO reactions come from two types of experiments: measurements of quantum yields in the chlorine-photosensitized decomposition of a source gas such as O_3, $C1_20$ or OC1O, and time-resolved experiments using flash photolysis, discharge-flow or molecular modulation which measure the concentrations of reactive intermediates such as C1O and C1OO as well as stable products. The results of both types of experiments will be discussed below.

Early flash photolysis studies of reaction 1 (Porter and Wright[3]; Edgecombe *et al.*[4]) concluded that the ClO + ClO reaction had only one product channel which formed $Cl_2 + O_2$ via the decomposition of a stabilized ClOOCl intermediate, *i.e.*,

$$ClO + ClO \leftrightarrow ClOOCl \text{ ------> } Cl_2 + O_2$$

Radical channels were not considered. While Edgecombe *et al.* observed the formation of OC1O in the photolysis of systems containing Cl_2O, this was ascribed to the reaction

$$ClO + Cl_2O \longrightarrow Oclo + Cl_2$$

rather than to a channel of the C1O + C1O reaction, Benson and Buss[40] argued that in order to account for the long chain lengths observed in photolytic decompositions of $C1_20$ and OClO, the self-reaction of C.1O must involve a step which produced atomic chlorine and a new species, ClOO:

$$ClO + ClO \text{ -------+ } Cl + ClOO$$

They also suggested that the termination of C1O in the flash photolysis experiments was due to the exothermic back-reaction of these species,

$$Cl + ClOO \longrightarrow Cl_2 + O_2$$

In their molecular modulation study, Johnston and co-workers[13] confirmed the involvement of the C1OO radical in this mechanism and concluded that both the Porter *et al.* and Benson and Buss mechanisms were important. Clyne and Coxon[10] observed emission from $C1_2(^3\Pi)(v\leq9)$ in their discharge-flow experiments and assumed that the Cl + C1OO reaction was the source, although later work showing that C1OO is less stable than previously thought casts doubt on this interpretation. In similar discharge-flow experiments using mass spectroscopic detection at low pressure, Clyne, McKenney and Watson[12] identified a reaction channel producing OClO, obtaining a branching ratio of about 0.05 at 298 K. Several groups have subsequently studied the C1O + ClO reaction using molecular modulation and have measured branching ratios $[k_2:k_3:k_4]$ for all three channels including Cox and Derwent[15] [0.50:0.34:0.16], Burrows and Cox[16] [0.35:0.31:0.34] and Simon *et al.*[18] [0.34:0.32:0.34]. The latter three studies were carried out in the presence of high concentrations of 0_2, which is known from quantum yield studies to have an effect on the branching ratios. Prior to this work, temperature dependences for the branching ratios have not been reported.

Information on the bimolecular-branching ratios has also been obtained from quantum yield studies. Both Lin *et al.*[19] and Wongdontri-Stuper *et al.*[41] measured quantum yields for O_3 destruction in the photolysis of Cl_2. At 298 K, both groups obtained quantum yields around 6 in the presence of N_2 buffer gas, implying that $k_3/k_2 \approx 2$. From simultaneous measurements of O_3 and OC1O, Wongdontri-Stuper *et al.* obtained branching ratios of 0.34, 0.63 and 0.032 for reactions 2, 3 and 4, respectively. These values are consistent with the results of Lin *et al.* The quantum yield can be related to the rate constants for reactions 2, 3 and 4 by the expression,

$$-\Phi_{O_3} = 2\left\{1 + \frac{k_3 + \frac{k_4}{2}}{k_2 + \frac{k_4}{2}}\right\}$$

From the absolute values of k_2, k_3 and k_4 reported in this study, a value for the quantum yield in N_2 buffer gas of 5.0 ± 1.2 may be calculated using the above expression. 'l'his is in reasonable agreement with the results of 1.in *et al.* and Wongdontri-Stuper *et* al.

Both Lin *et al.* and Wongdontri-Stuper *et al.* observed that the quantum yield decreased rapidly with temperature, reaching the limiting value of 2 at temperatures between -20° C and 0° C. As discussed by Watson, this dependence on temperature is too large to be explained by the temperature dependences of the elementary reaction channels. With recent improvements in the understanding of the stability of chlorine peroxide, it now seems likely that the observed temperature dependence of the quantum yield is influenced by secondary reactions involving C1OOC1, *i.e.*,

$$ClO + ClO \xrightarrow{M} ClOOCl$$

$$Cl + ClOOCl \longrightarrow Cl_2 + ClOO$$

$$Cloo \xrightarrow{M} cl + O_2$$

Net: $C1O + C1O \longrightarrow C1_2 + 0_2$

This mechanism is equivalent to the CIOOC1-catalyzed termination of C1O, a process which effectively increases k_2 and therefore reduces the quantum yield at temperatures below 25° C where C1OOC1 becomes increasingly stable.

Atmospheric implications. Sander *et al.*[7] have discussed the implications of the present measurements of k_1 at low temperatures for ozone destruction in the springtime polar stratosphere.

In the nighttime polar vortex in the Southern Hemisphere, the atmosphere is frequently denitrified duc to the condensation and sedimentation of polar stratospheric cloud particles. Under these conditions, the partitioning of active chlorine is determined by the rates of formation and thermal decomposition of C1OOC1. Values for k. 1 from the present work extrapolated to stratospheric temperatures arc more than a factor of three smaller than those derived from the work of Cox and 1 layman.[20] and equilibrium constants for reaction 1 arc correspondingly larger. The predicted nighttime concentrations of ClO in equilibrium with ClOOCl will therefore bc about 40% smaller than the previous kinetic data would suggest. in darkness, however, the thermal lifetime of ClOOCl at 50 mb is about 11 days, and under most conditions of polar atmospheric transport, ClO will not thermally equilibrate with its dimer before encountering sunlight, which dissociates ClOOCl on a much more rapid time scale.

The kinetic measurements reported here indicate that all the bimolecular channels have significant activation energies. These reactions can therefore play no role in the stratosphere where the temperatures arc sufficiently low that the termolecular channel always dominates.

summary

Rate constants were measured for bimolecular and termolecular channels of the ClO + ClO reaction. The following results were obtained:

1. *Formation and Thermal Decomposition of ClOOCl:* The Arrhenius expressions for the formation and thermal decomposition of ClOOCl in the low pressure limit (M = N2) were determined to be $k_1(T)$ =- (1 .22* 0.15)x 10^{-33} exp{(833 ± 34)/1'} cm^6 $molecule^{-2}$ s^{-1} and $k_{-1}(T)$ = (9.81 ± 1.32) x 10-7 exp{-(7980 ± 320)/'1'} cm^3 $molecule^{-1}$ S-l, respectively. From falloff data obtained below 250 K, $k_{1,\infty}$ was determined to be (6 ± 2) x 10^{-12} cm^3 $molecule^{-1}$ s^{-1}, independent of temperature. The expression for the C1O-C1OOCI equilibrium constant is $K_{eq}(T)$ = (1.24 ± 0.18) x 10^{-27} exp{(8820 ± 440)/T} cm^3 $molecule^{-1}$."l-his expression was derived from a 3rd Law analysis of the equilibrium constant data. Equilibrium constants from this work extrapolate to values that are about a factor of three larger than the present NASA recommendations at polar stratospheric temperatures.

2. *Third-Body Dependencies:* The rate coefficients for C1OOC1 formation as a function of bath gas at 298 K in the low-pressure limit arc (0.99 ± 0.05) x 10^{-32}, (1.24 ± 0.09) x 10^{-32}, (1.71 ± 0.06) x 10^{-32}, (2.00 ± 0.27) x 10-32, (2.60 ± 0.1 7)x 10^{-32}, (3.15 ± 0.14) x 10^{-32} and (6.7 ± 3.7) x 10^{-32} cm^6 $molecule^2$ s^1 for He, 0_2, Ar, N_2, CF_4, SF_6 and Cl_2, respectively. The low value for 0_2 relative to Ar and N_2 may indicate that 0_2 plays a greater role in the formation of ClOOCl than as a collision partner. The large value for $C1_2$ as a third body is attributed to a chaperone mechanism in which a C10-$C1_2$ intermediate catalyzes the formation of ClOOCl. 'l'his effect

may be responsible for the non-zero intercept observed by Trolier *et* al. at low temperatures in the low-pressure limit.

3, *Bimolecular Reaction Channels:* Rate coefficients for the bimolecular channels are $k_{Cl_2+O_2}(T) = (1.013 \pm 0.12) \times 10^{-12} \exp\{-(1590 \pm 100)/T\}$ cm^3 molecule^{-1} S-l, $k_{ClOO+Cl}(T) = (2.98 \pm 0.68) \times 10^{-11} \exp\{-(2450 \pm 450)/T\}$ cm^3 molecule^{-1} S-l and $k_{OClO+Cl}(T) = (3.50 \pm 0.31) \times 10^{-13} \exp\{-(1370 \pm 150)/T\}$ cm3 molecule^{-1} s-', The room temperature branching ratio is $k_{Cl_2+O_2}$: $k_{ClOO+Cl}$: $k_{OClO+Cl}$ = 0.29:0.50:0.21 and the value for the overall rate constant ($k_{Cl_2+O_2}$ + $k_{ClOO+Cl}$ + $k_{OClO+Cl}$) at 298 K is (1 .642 0.35)x 10-14 cm^3 molecule^{-1} S-l.

4. *Thermochemistry:* Enthalpies of formation for ClOOCl and OClO were calculated to be $\Delta H^o_{f,ClOOCl}(298) = 30.5 \pm 0.7$ kcal mol^{-1} and $\Delta H^o_{f,OClO}(298) = -22.6 \pm 0.3$ kcal mol^{-1}.

Acknowledgments

We thank Y. L.. 1 la and Y. L.. Yung for their assistance in the development of the computer code for mechanism fitting and W. B. DeMore for many stimulating discussions. We also thank G. Smith (SRI International) for the usc of his thermodynamics codes. The research described in this paper was carried out at the Jet Propulsion Laboratory, California Institute of Technology, under contract to the National Aeronautics and Space Administration.

References

1. Finkelnburg, W.; Schumacher, 1 I. J.; Stieger, G. Z *Physik. Chem. 1931, B15*, 127,

2. Norrish, R. G. W.; Neville, G.H.J. *J. Chem. Sot.* **1934**, 1864.

3. Porter, G.; Wright, F.J. *J. Chem. Soc., Fara. Disc. 1953,* 14,23.

4. Edgecombe, F.H.C.; Norrish, G. G. W.; Thrush, B.A. *Proc.* Roy Sot, *(London)* 19S7, *A243*, 24.

5. Basco, N.; Dogra, S.K. *Proc. R. Soc. London, Ser. A 1971,323,29.*

6. Basco, N.; Hunt, J.E. *Int. J, Chem. Kinet. 1979,9,649.*

7. Sander, S. P,; Friedl, R.R.; Yung, Y. I,. Science **1989**, 245, 1095.

8. Trolier, M.; Mauldin 111, R.L.; Ravishankara, A.R. *J. Phys. Chem.* 1990, 94,4896,

9. Clyne, M. A. A.; Coxon, J.A. *J. Chem. Soc., Fara. Trans. 1966, 62, 1175.*

10. Clyne, M. A. A.; Coxon, J.A. *Proc. R. Sot. London, Ser. A 1968,303,207.*

11. Clyne, M. A. A.; White, I.F. *J. Chem. Soc., Fara. Trans. 1* **1971**, *67,2068.*

12. Clyne, M, A, A.; McKcnncy, D.J.; Watson, R.T. *J. Chem. Soc., Fara. Trans.*] **1975**, *71*, 322.

13. Johnston, 11. S.; Morris, E.D.; Van den Bogaerde, J. *J. Am. Chin. Soc.* 1969, 91, 7712.

14! Cox, R. A.; Derwent, R.G.; Eggleton, A.E.; Reid, H.J. *J. Chem. Sot., Fara. Trans. 1 1979,* 75, 1648.

15. Cox, R. A,; Derwent, R.G. *J. Chem. Sot., Fara. Trans. 1 1979,* 75, 1635.

16. Burrows, J. P.; Cox, R.A. *J. Chem. Sot., Fara. Trans. 11981, 77,2465.*

17. I layman, G. D.; Davies, J. M.; Cox, R.A. *Geophys. Res. Lett.* 1986, *13, 1347*

18. Simon, F.G.; Schneider, W.; Moortgart, G. K.; Burrows, J.P. *J. Photochem. Photobiol. A: Chem. 1990,55,* 1.

19, Lin, C.L.; Jaffe, S.; DeMore, W.B. *"Photochemistry of chlorine-ozone mixtures"*, American Chemical Society, 169th National meeting, Philadelphia, **1975**.

20. Cox, R. A.; 1 layman, G. Il. *Nature 1988,332, 796.*

21. Sander, S. P.; Friedl, R.R. J. *Phys. Chem. 1989,93,4764.*

22. Watson, R.T. *J. Phys. Chem. Ref. Data* **1977**, 6, 908.

23. Burkholder, J.B.; Orlando, J. J.; 1 loward, C.J. *J. Phys. Chem.* 1990, 94,687.

24. Okabe, 11. *Photochemistry of Small Molecules*, John Wiley & Sons, Ncw York, 1978.

25. Wahncr, A.; Tyndall, G. S.; Ravishankara, A. I<, *J. Phys. Chem.* 1987, 91,2734.

26. DeMore, W. R.; Sander, S.1'.; Golden, D.M.; Hampson, R.F.; Kurylo, M. J.; Howard, C. J.; Ravishankara, A.R.; Kolb C.E.; Molina, M.J. *"Chemical Kinetics and Photochemical Data for Use in Stratospheric Modeling--Evaluation Number 10"*, JPL Publication 92-20, Jet Propulsion Laboratory, California Institute of Technology, Pasadena, CA.

27. Cady, G.H. *Inorg. Syn.* 1967, S, 156.

28. a) '1'roe, J. *J. Chem. Phys. 1977,66, 4745;* b) '1'roe, J. *J. Chem. Phys.* 1977, *66, 4758; c)* Patrick, R.; Golden, D.M. *Int. J. Chem. Kinet* 1983, *15*, 1189.

29. Curtis, A. R,; Sweetenham *"FACSIMILE/CHEKMA* T", U.K. Atomic Energy Authority, Harwell 1987.

30. Chase, M. W., Jr.; Davies, C. A.; Downey, J. R., Jr.; Frurip, D. J.; McDonald, R. A.; Syverud, A.N. *"JANAF Thermochemical Tables", J. Phys. Chem. Ref. Data* **1985**, *14*.

31. Cheng, B. M.; lee, Y, I'. *J. Chem. Phys. 1989,* 90, 5930,

32. Birk, M.; Fried], R.R.; Cohen, E.A.; Pickett, H. M.; Sander, S.P. *J. Chem. Phys.* 1989, *91, 6588.*

33. Rendell, A.P.; Lee, T.J. *J. Chem. Phys.* 1991,94,6219.

34. Benson, S.W. *'Thermochemical Kinetics",* 2nd ed., John Wiley and Sons, Ncw York, 1976.

35. Bunte, S. *Private communication.*

36. Lee, T. J.; Rohlfing, C. M.; Rice, J. E. *J. Chem. Phys. 1992,97,6593.*

37. Rochkind, M. M.; Pimentel, G.C. *J. Chem. Phys. 1965,42, 1361.*

38. Rochkind, M. M.; Pimentel, G.C. J. *Chem. Phys.* 1967,46,4481

39. Chi, F.K.; Andrcws, 1,. *J. Phys. Chem. 1973, 77, 3062.*

40. Benson, S. W.; Buss, J. Il. *J. Phys. Chem.* 1957,27, 1382,

41. Wongdontri-Stuper, W.; Jayanty, R. K.M.; Simonaitis, R.; Heicklen, J. *J. Photochem.* **1979**, *10*, 163.

42. IUPAC, Evaluated Photochemical Data for Atmospheric Chemistry: Supplement 111, *J. Phys. Chem. Ref. Data 1989,89, 889.*

Table I. Summary of reactions used in fitting of data to the reaction mechanism.

	Reaction	Rate coefficient	Experimental conditions		
			xs Cl_2O	Xs Cl	XS Cl_2O
			Temp = 195-250	250-400	250-400
initiation:	c1 + Cl_2O ⟶ ClO + Cl_2	$k_5 = 9.9 \times 10^{-11}$ *b*	■	■	■
termolecular channel:	C1O + ClO $\xrightarrow{M}$ C1OOCI	k_1 *a*	■	■	■
	ClOOCl $\xrightarrow{M}$ ClO + C1O	$k_{-1} = 6.3 \times 10^{-6} \{T/300\}^{-3.6} \exp\{-8450/T\}$ *b*	❑	■	■
bimolecular channels:	C1O' ClO ⟶ Cl_2 + 02	k_2 *a*	❑	■	■
	ClO + ClO — - , ClOO + Cl	k_3 *a*	❑	■	❑
	ClOO + Cl ⟶ $Cl_2 + O_2$	$k'_{-3} = 1.4X\ 10^{-10}$ *b*	❑	■	•1
	⟶ ClO + ClO	$k''_{-3} = S.0 \times 10^{-12}$ *b*	❑	■	c!
	ClO + ClO ⟶ OClO + Cl	k_4 *a*	El	■	■
	OClO + Cl ⟶ Clo -'- ClO	$k_{-4} = 3.4 \times 10^{-11} \exp\{160/T\}$ *b*	•1	■	❑

Table I (con *t.*).

	Reaction	Rate coefficient	Experimental conditions: Xs Cl_2O, Temp = 195-250	Xs Cl, 250-400	Xs Cl_2O, 250-400
secondary chemistry:	$ClOOCl + Cl \longrightarrow ClOO + Cl_2$	$k_6 = 1.0 \times 10^{-10}$ *b*	❑	■	•1
	$CI402 \xrightarrow{M} ClOO$	$k_7 = 2.7 X 10^{-33}\{T/300\}^{-1.5}$ *b*	❑	■	❑
	$ClOO \xrightarrow{M} c1 + O_2$	$k_{-7} = 4.7x\ 10^{-9}\{T/300\}^{-1.5} \exp\{-2500/T\}$ *b*	•l	■	❑
	$cl + ClO \xrightarrow{M} Cl_2O$	$k_8 = 6 \times 10^{-32}$ *d*	❑	■	❑
	$cl + c1 \xrightarrow{M} Cl_2$	$k_9 = 7.5 \times 10^{-34} \exp\{906/T\}$ *c*	❑	■	❑
mass transport:	C1O. C1OOCI, etc. $\longrightarrow$ leave cell	$\tau_{flow} = 0.01 - 0.1$	❑	■	■

a) determined in fitting procedure.
b) from reference 26.
c) from reference 36.
d) estimated using Tree's method (see text).
e) ■ indicates reaction used in fitting routine--El indicates reaction not used in fitting routine.

Table II. Summary of conditions for each set of experiments and absorption cross sections.

Temperature (K)	$[Cl_2O]$ (cm^3 $molecule^{-1}$)	$[Cl_2]$ (cm^3 $molecule^{-1}$)	[Cl] (cm^3 $molecule^{-1}$)	[M] (cm^3 $molecule^{-1}$)
Excess Cl_2O:				
195-250	1.0- 1.5x1015	2. O-5. OX1O15	$2.0 - 5.0 \times 10^{13}$	$1 - 30 \times 10^{18}$
Excess *Cl*:				
250-400	$4-8 \times 10^{13}$	$5 - 18 \times 10^{16}$	$2 - 7 \times 10^{14}$	0.5 -6x1018
Excess Cl_2O:				
250-400	$1.0- 1.5 \times 10^{15}$	1.0- 1.2X1016	$4.0 - 5.0 \times 10^{13}$	0.5 -22x1018

Absorption cross sections at 275.5 nm (298 K):

$\sigma_{ClO} = 8.4 \times 10^{-18}$ cm^2 $molecule^{-1}$ $\sigma(T) = \sigma(298)\{1.011 - 104.9/T + 30330/T^2\}$

$\sigma_{Cl_2O} = 1.24 \times 10^{-18}$ cm^2 $molecule^{-1}$

$\sigma_{ClOOCl} = 2.45 \times 10^{-18}$ cm^2 $molecule^{-1}$

$\sigma_{Cl_2} = 2.19 \times 10^{-20}$ cm^2 $molecule^{-1}$

Table 111. Summary of experimental rate coefficients, k_1, as a function of N_2 concentration under conditions of excess Cl_2O and T < 250 K, and results of fits to 'l'roe's fall-off expression.[a]

Temp. (K)	$10^{-18} \times [N_2]$ (molecule cm^{-3})	$10^{13} \times k_1$ (cm^3 $molecule^{-1}$ s^{-1})	$10^{32} \times k_0$[b] (cm^6 $molecule^{-2}$ s^{-1})	$10^{12} \times k_\infty$[c] (cm^3 $molecule^{-1}$ s^{-1})
195	1.00	0.81	8.8	3.8
	1.25	0.94		
	1.67	1.22		
	2.50	1.70		
	2.62	1.75		
	3.00	1.88		
	4,23	2.51		
	5.00	2.94		
	6.94	3.72		
	10.0	4,80		
	11.3	5.59		
	18.2	7.77		
208	1,00	0.67	6.6	7
	1.62	0.96		
	2.65	1.58		
	4.27	2.28		
	6.98	2.98		
	11.4	4,72		
	18.4	8.22		
	30,0	11,2		
220	1.00	0.48	5.3	6
	1.61	0.75		
	2,65	1.29		
	3.00	1.36		
	4.28	1.90		
	6.91	2.72		
	11.4	3,87		
	18.4	5.85		
	30.0	9.64		

Table 111 (*con* 't.).

Temp. (K)	10^{-18} x [N_2] (molecule cm^{-3})	10^{13} x k_1 (cm^3 molecule-l s-l)	10^{32} X k. (cm^6 $molecule^{-2}$ s^{-1})	10^{12} x k_∞ (cm^3 $molecule^{-1}$ S-l)
233	1.00	0.43	4.6	5
	1.62	0.68		
	2.65	1.01		
	4.28	1.58		
	6.98	2.45		
	11.4	3.49		
	18.4	5.05		
	30.1	7.96		
247	1.00	0.31	3.7	7
	1.62	0.53		
	2.65	0.80		
	3.00	1.04		
	4.28	1.48		
	6,98	2.13		
	11.5	3.15		
	18.4	5.00		
	30.0	6.73		

a) The fall-off equation is given by:[28]

$$k([M],T) = \frac{k_0[M]}{1+\frac{k_0[M]}{k_\infty}} F_c^{\{1+[\log_{10}(k_0[M]/k_\infty)]^2\}^{-1}}$$

b) k_0 was determined by fitting the data at each temperature to the fall-off equation. Fitting $k_0(T)$ to the expression, $k_0(T) = k.300\ (T/300)$-n yielded $k_0 300 = (1.8 \pm ().5) \times 10^{-32}$ cm^6 $molecule^{-2}$ S-l and n = 3.6 ± 1.0.

c) k_∞ was determined by fitting the data at each temperature to the fall-off equation. Fitting $k_\infty(T)$ to the expression, $k_\infty(T) = k_\infty^{300}\ (1'/300)^{"}1$ yielded $k_\infty 300 = (6,() \pm 2.0) \times 10^{-12}$ cm^3 molecule-l s^{-1} and m = 0,0 ± 1.0.

'J'able IV. Summary of ClOOCl formation rate coefficient data with N_2 as a bath gas.

Temperature (K)	$10^{32} \times k_1$ (cm^6 molecule"] s^{-}])
195	8.8 ± 1.8
208	*6.6* ± 1.3
220	5.3 ± 1.1
233	4.6 ± 0.9
247	3.7 ± 0.7
260	2.60 ± 0.70
270	2.48 ± 0.23
280	2.38 ± 0.33
290	2.23 ± 0.14
300	2.07 ± 0.27
310	1.75 ± 0.10
330	1 ,59* 0.09
350	1,38 ± 0.03
360	1.24 ± 0.24
370	1.13 ± 0.22
380	1.09 ± 0.22
390	0.99 ± 0.49

l'able V. Summary of bimolecular rate coefficient data as a function of $[Cl_2]$ under excess chlorine atom conditions.

Temperature (K)	$10^{-16} \times [Cl_2]$ (molecule cm^{-3})	$10^{14} \times (k_2 + k_3 + k_1'[Cl_2])$ (cm^3 $molecule^{-1}$ s^{-1})	$10^{14} \times (k_2 + k_3)$ (cm^3 $molecule^{-1}$ s^{-1})
270	5.15	1.68	0.44 ± 1.34
	5.80	1.96	
	7.61	2.05	
	9.94	1.74	
	14.56	3.95	
280	5.09	1.65	1.02 ± 0.70
	5.86	1.78	
	7.47	1.90	
	9.82	2.41	
	12.63	1.96	
	14.80	3.19	
	14.81	2.83	
290	5.11	1.88	0.90 ± 0.82
	7.55	1.82	
	9.95	2.05	
	12.41	2.35	
	14.75	3.30	
300	5.00	1,94	1.66 ± 0.42
	7.24	2.03	
	9.78	2.59	
	14.52	2.55	
	17.17	2.79	
310	5.13	2.48	*1.92 ± 0,27*
	7.56	2.43	
	9.96	2.81	
	14.57	3.12	
	17.83	3.53	
330	5.17	3.87	*3.48 ± 0.20*
	7.62	4.14	
	10.05	4.36	
	12.53	4.48	

Table v (cm *t.).*

Temperature (K)	10-]6 x [Cl_2] (molecule cm^{-3})	10^{14} x (k_2 + k_3 + k_1'[Cl_2]) (cm^3 molecule" ^{1} S-l)	1 0^{14} X (k_2 + k_3) (cm^3 $molecule^{-1}s^{-1}$)
350	5.22	4.38	3.993.0.39
	7.63	4.80	
	10.08	4.98	
	12.53	5.31	
	14,63	5.24	
360	5.07	4.90	4.43 ± 0.32
	7.52	4.94	
	14.53	5.61	
370	*6.04*	*5.49*	*4.28* ± 1.38
	8.99	*5.99*	
	11.34	*6.43*	
	13.53	*7.58*	
	14.95	*6.84*	
380	5.11	6.46	*5.36 ± 0.81*
	7.51	6.67	
	10.03	6.84	
	12.36	7,29	
	15.13	8.32	
390	5.04	9.13	7.59 ± 2.96
	7.55	9.72	
	10.17	12.97	
	12.53	11.54	
	15.43	12.84	

Table VI. Summary of k_1 for different bath gases obtained under excess Cl conditions.

Bath Gas	Temp. (K)	$10^{32} \times k_1$ (cm^6 $molecule^{-2}$ s^{-1})
He	300	0.99 ± 0.05
O_2	300	1.24 ± 0.09
Ar	300	1.71 ± 0.06
N_2	300	1.96 ± 0.24
CF_4	300	2,60 ± 0.17
SF_6	300	3.15 ± 0.14
Cl_2	260	15.9 ± 7.7
	270	21.3 ± 14.4
	280	12.2 ± 6.5
	290	13.9 ± 8.9
	300	6.7 ± 3.6
	310	8.6 ± 2.3
	330	8.3 ± 2.1
	350	9.5 ± 3.7
	360	8.0 ± 3,2
	370	19.9 ± 12.1
	380	17.5 ± 7.6
	390	36.0 ± 27.5

Table VII. Summary of ClO + ClO → Cl_2 + O_2 and ClO + C1O → OC1O + Cl rate coefficient data obtained under excess Cl_2O conditions.

Temp. (K)	$10^{15} \times k_2$[a] ($cm^3 molecule^{-1} s^{-1}$)	$10^{15} \times k_4$[a] ($cm^3 molecule^{-1} s^{-1}$)	$10^{15} \times (k_2 + ½k_4)$[a] ($cm^3 molecule^{-1} s^{-1}$)	$10^{15} \times (k_2 + ½k_4)$[b] ($cm^3 molecule^{-1} s^{-1}$)
300	5.19 ± 0.24	3.29 ± 0,09	6.84	---
310	6.06 ± 0.27	4.43 ± 0.31	8.27	---
320	6.59 ± 0.08	5.15 ± 0.28	9.16	---
330	8.09 ± 0.20	5.56 ± 0.18	10.87	---
340	9,28 ± 0.40	6.25 ± 0,47	12.40	11.53 ± 0.20
350	10.70 ± 0.36	6.97 ± 0.31	14.18	---
360	12.19 ± 0.27	7.70 ± 0.40	16.04	---
370	13.88 ± 0.61	8.62 ± 0.58	18.19	19.13 ± 0.73
380	15.50 ± 0.73	9.22 ± 0.53	20.11	---

a) determined from OC1O formation data.
b) determined from C1O loss data,

Table VIII. Summary of ClOOCl decomposition rate coefficient and equilibrium constant data.

Temperature (K)	$10^{20} \times k_{-1}$ (cm^3 molecule^{-1} s^{-1})	$10^{-5} \times K_p$ (atm^{-1})
260	3.96 ± 0.84	213.5 ± 47.9
270	11.5 ± 2.30	62.84 ± 13.25
280	38.2 ± 2.47	16.32 ± 1.08
290	130.3 ± 12,0	4,171 ± 0.394
300	304.4 ± 20.6	1.568 ± 0.109
310	823.5 ± 101.2	0.513 ± 0.065

Figure Captions

Figure 1. Time-dependent absorption signal under conditions of excess chlorine atoms measured with a PMT at 275.5 nm. (a) Signal fit to the entire reaction mechanism including dirner decomposition, secondary chlorine chemistry and flow through the cell. (b) Signal fit to a simple second order mechanism. The difference between the full mechanism and the second order mechanism fits is slight, but can been seen in the greater variation of the residuals of the second order fit from the experimental data. The difference in the calculated k_{tot} between the two fits is 15%.

Figure 2. k_{tot} (= k_1 [N_2] + k_2 + k_3) versus N_2 concentration as a function of Cl_2 concentration at 1' = 350 K, [Cl_2] = 5.22 x 10^{16} molecule cm^{-3} (■), 7.63 x 10^{16} molecule cm^{-3} (□), 10.08 x 10^{16} molecule cm^{-3} (A), 12.53 x 10^{16} molecule cm^{-3} (△) and 14.63 x 10^{16} molecule cm^{-3} (.). Slopes give k_{1,N_2}, and y-intercepts give (k_2 + k_3 + k_{1,Cl_2}[Cl_2]).

Figure 3. y-intercepts of Figure 2 versus Cl_2 concentration. The slope gives k_{1,Cl_2}, and the y-intercept gives (k_2 + k_3).

Figure 4. (a) Arrhenius plot of k_{1,N_2}. Open points (○) were measured under conditions of excess Cl_2O. Solid points (.) were measured under conditions of excess chlorine atoms. Resulting rate constant expression is $k_{1,N_2}(T)$ = (1 .22 ± O, 15) x 10-33 exp{(833± 34)/T} cm^6 $molecule^{-2}$ S-l. (b) Plot of ln[k_{1,N_2}] vs. ln[T/300]. linear fit resulted ink] $_{,N_2}(T)$ = (2.07 ± 0.09)x 10-32 {T/300 }-3001 $^{\pm 0.20}$ cm^6 $molecule^{-2}$ s-'.

Figure 5. Arrhenius plots of bimolecular rate constants. Fits yielded (k_2 + k_3)(T) = (1 .78 ± 0.38) x 10^{-11} exp{-(2150 ± 450)/T} cr^{n3} molecule-l s^{-1} (■), $k_2(T)$ = (1 .01 ± 0.12) x 10^{-12} exp{-(1590 ± 100)/T} cm^3 molecule-l S-* (.) and $k_4(T)$ = (3.50 ± 0.31) x 10^{-12} exp{-(1370 ± 150)/T} cm^3 $molecule^{-1}$ S-l (A).

Figure 6. k_{tot} (= k_1 [M] + k_2 + k_3) as a function of bath gas at 298 K. M = I Ic (.), O_2 (○), Ar (■), N_2 (□), CF_4 (A) and SF_6 (△). Slopes yield $k_{1,M}$ (see Table VI).

Figure 7. Time-dependent OC1O concentration under conditions of excess Cl_2O measured with an OMA. Each point on the OC1O curve is the result of fitting a 1024 point spectrum recorded by the OMA to a calibrated OC1O spectrum. Residuals indicate difference between measured [OClO] and that calculated in the analysis procedure. Inset plot shows an example fit of an experimental spectrum to a calibrated spectrum,

Figure 8. Time-dependent ClO concentration under conditions of excess Cl_2O measured with an OMA. Each point on the C1O curve is the result of fitting a 200 point spectrum recorded by the OMA to a calibrated C1O spectrum. Residuals indicate difference between measured [C1O] and that calculated in the analysis procedure. Inset plot shows an example fit of an experimental spectrum to a calibrated spectrum.

Figure 9. C1O-ClOOCl van't Hoff plot. (●) are the data determined in this study, and (△) are the data of Cox and Hayman.[20] The solid line indicates the 3rd Law fit to the data, and has a slope of9100 K. The dashed line is the 2nd Law analysis of the data and has a slope of 9820 K and a y-intercept of -20.8. The dash-dot line is the 2nd Law fit reported by Cox and Hayman and has a slope of **8710** K and a y-intercept of -17.3.

Figure 10, Sensitivity plot for the determination of k_{tot}. The abscissa indicates rate coefficients of the reaction mechanism which were held fixed in the fitting procedure when determining k_{tot}. Values in parentheses indicate the uncertainty in the canonical value of each rate coefficient. The ordinate indicates the percent change in the calculated value of k_{tot} when each rate coefficient is changed by the uncertainty factor. Filled bars show the change when rate coefficients are varied by +uncertainty factors, and open bars show the change when rate coefficients are varied by -uncertain y factors.

Figure 11. Sensitivity plot for the determination of bimolecular rate coefficients under conditions of excess Cl_2O. The left panel indicates the sensitivity in the

determination of k_2, and right panel indicates the sensitivity in the determination of k_4. (See Figure 10 caption for an explanation of plot.)

Figure 12. Sensitivity plot for the determination of the rate coefficient of ClOOCl dissociation. (See Figure 10 caption for an explanation of plot,)

Figure 13. ClO + C1O energy diagram. Energy is given in units of kcal me]$^{-1}$. Enthalpies of C1OOCI and OC1O and activation energies for the three bimolecular channels were determined in this study. Enthalpies of formation for ClO, $0_2(^1A)$ and $Cl_2(^3\Pi)$ were taken from ref. 30. The enthalpy of formation for ClOO was taken from ref. 26,

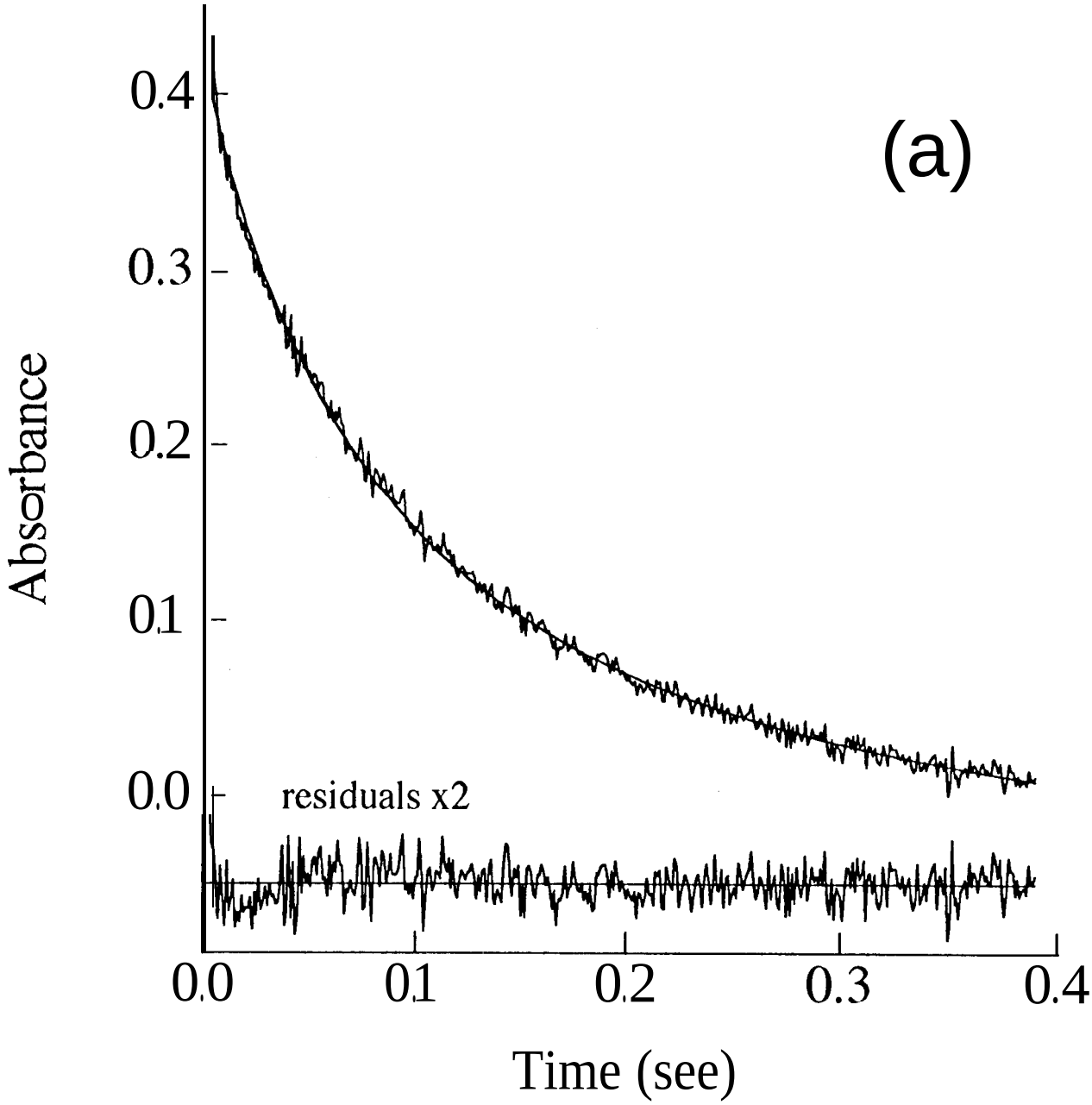
(a)
Absorbance
0.4
0.3
0.2
0.1
0.0
residuals x2
0.0
0.1
0.2
0.3
0.4
Time (see)

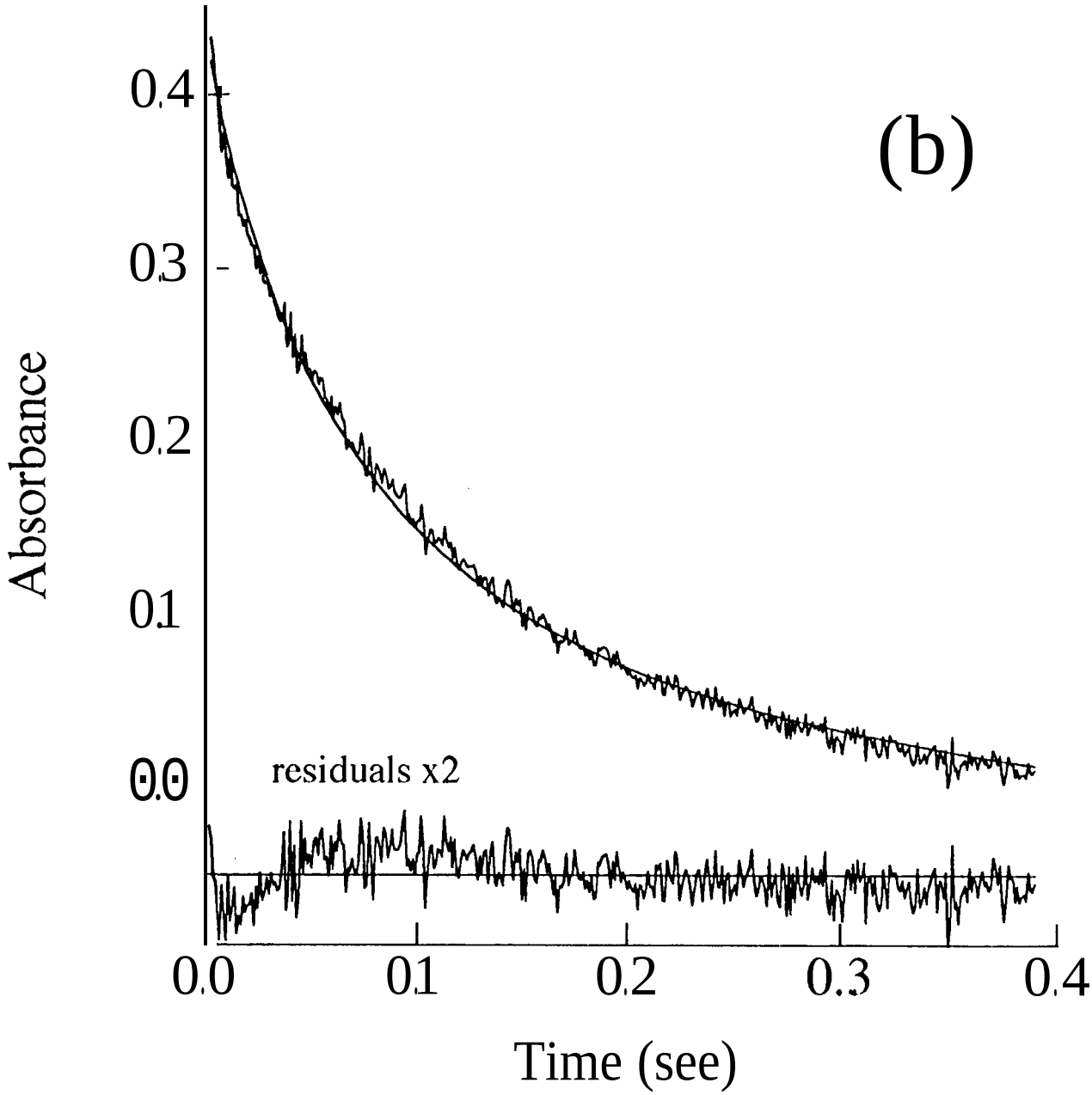
(b)
Absorbance
0.4
0.3
0.2
0.1
0.0
residuals x2
0.0
0.1
0.2
0.3
0.4
Time (see)

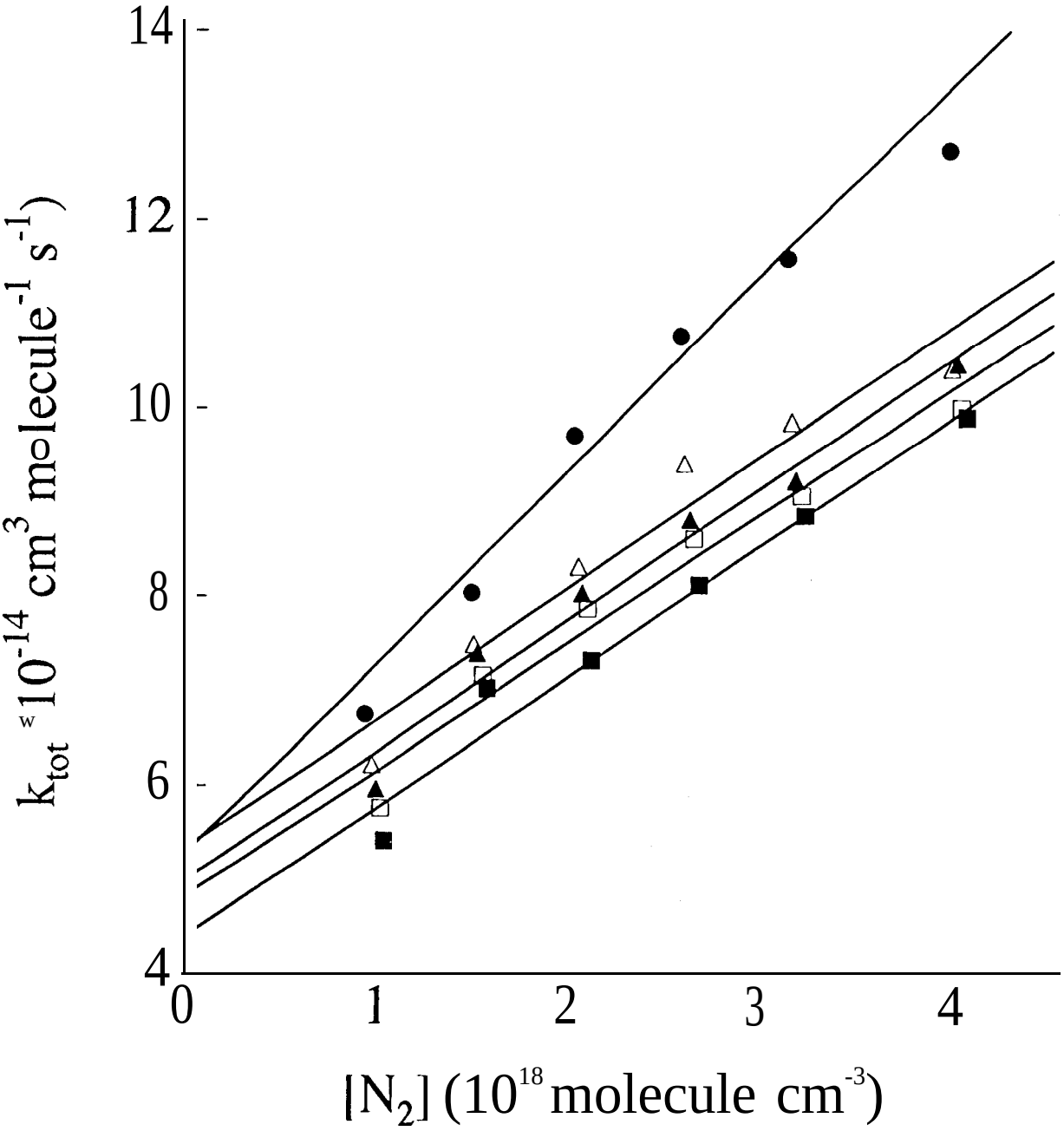
14
12
10
8
6
4
0
1
2
3
4
k_{tot} $^{w}10^{-14}$ cm^3 molecule^{-1} s^{-1})
[N_2] (10^{18} molecule cm^{-3})

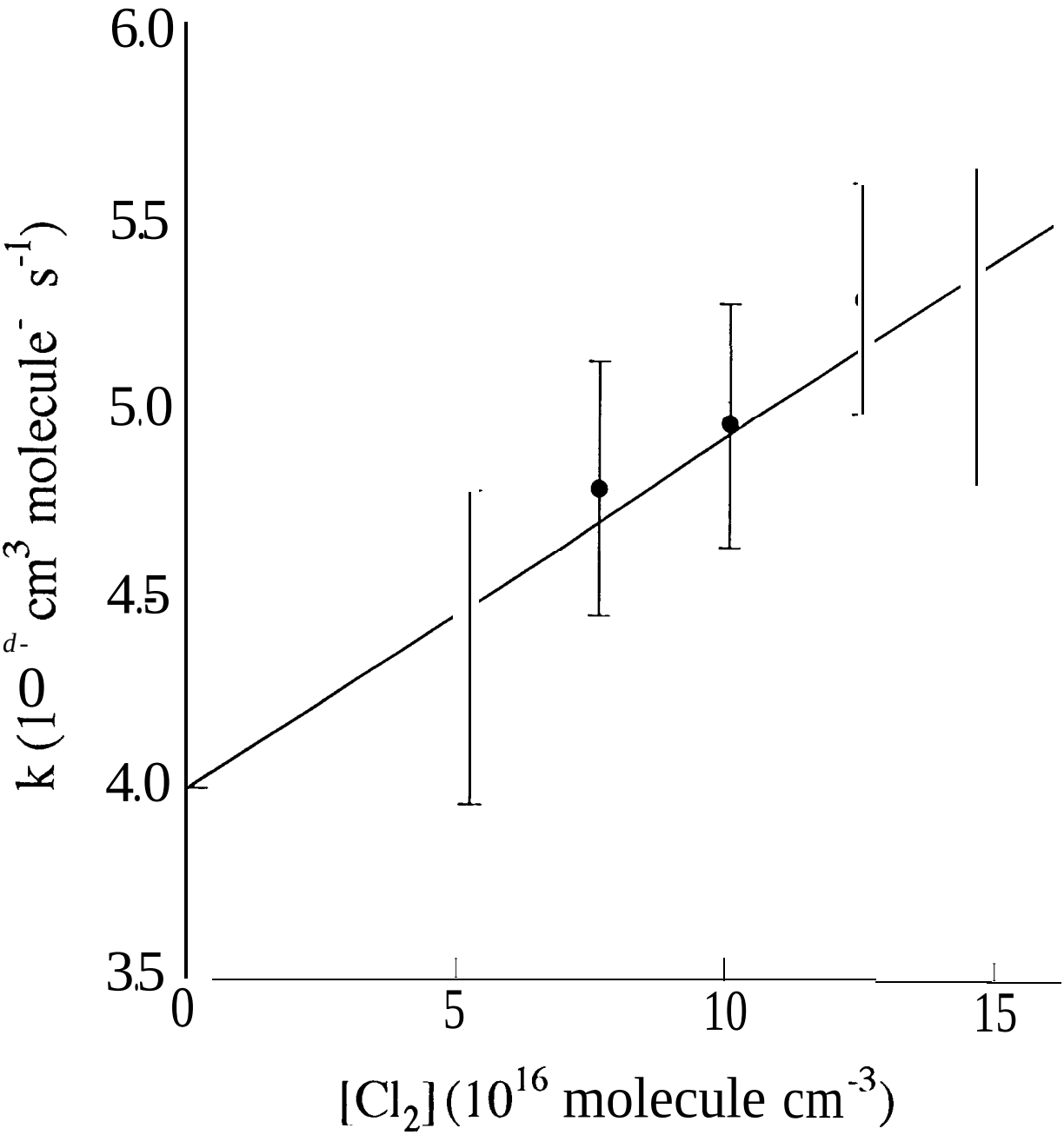
6.0
5.5
5.0
4.5
4.0
3.5
0
5
10
15
k (10^-d cm^3 molecule^-1 s^-1)
[Cl2] (10^16 molecule cm^-3)

Fig. 3

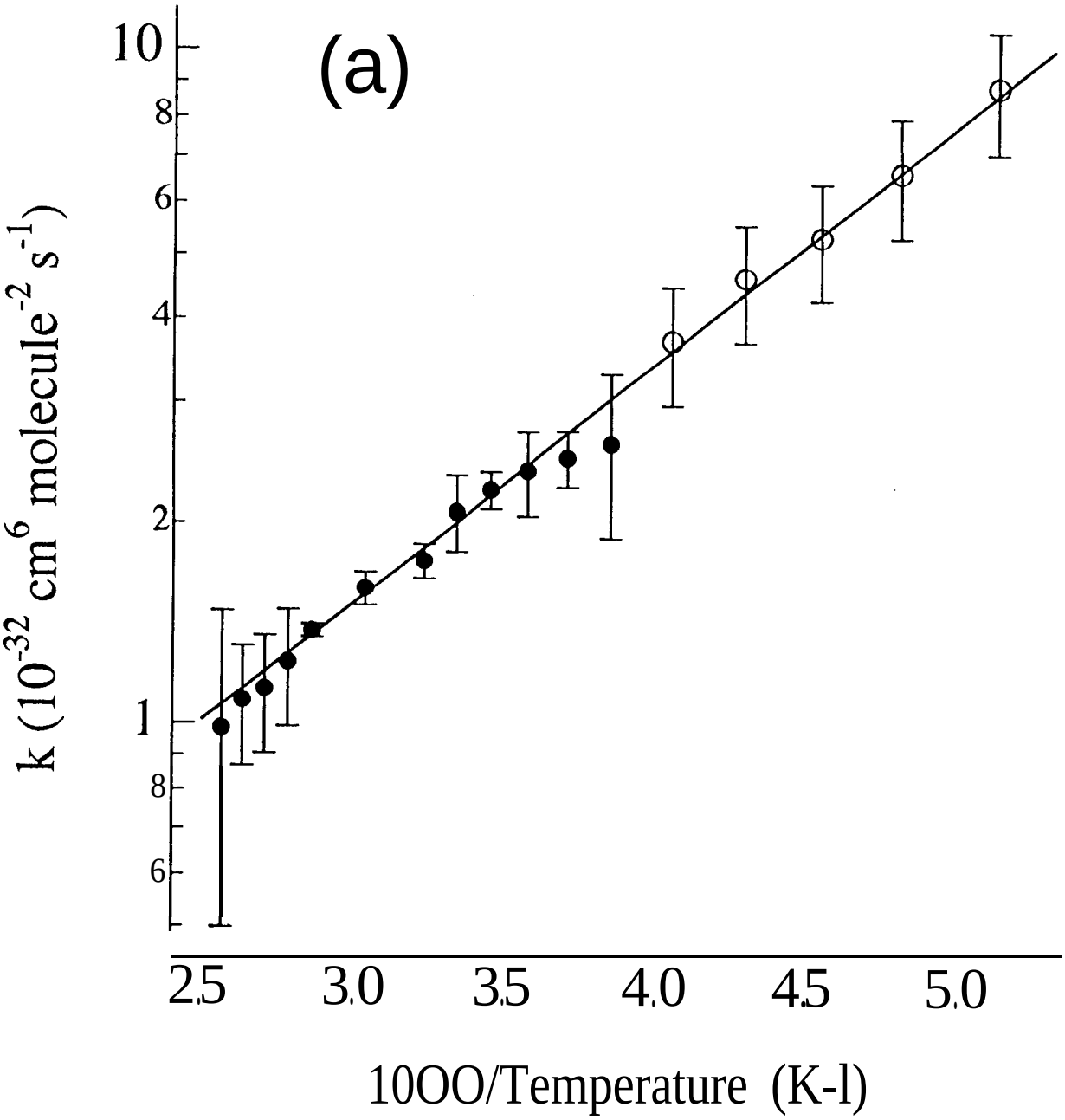
(a)
10
8
6
4
2
1
8
6
k (10^-32 cm^6 molecule^-2 s^-1)
2.5
3.0
3.5
4.0
4.5
5.0
10OO/Temperature (K-l)

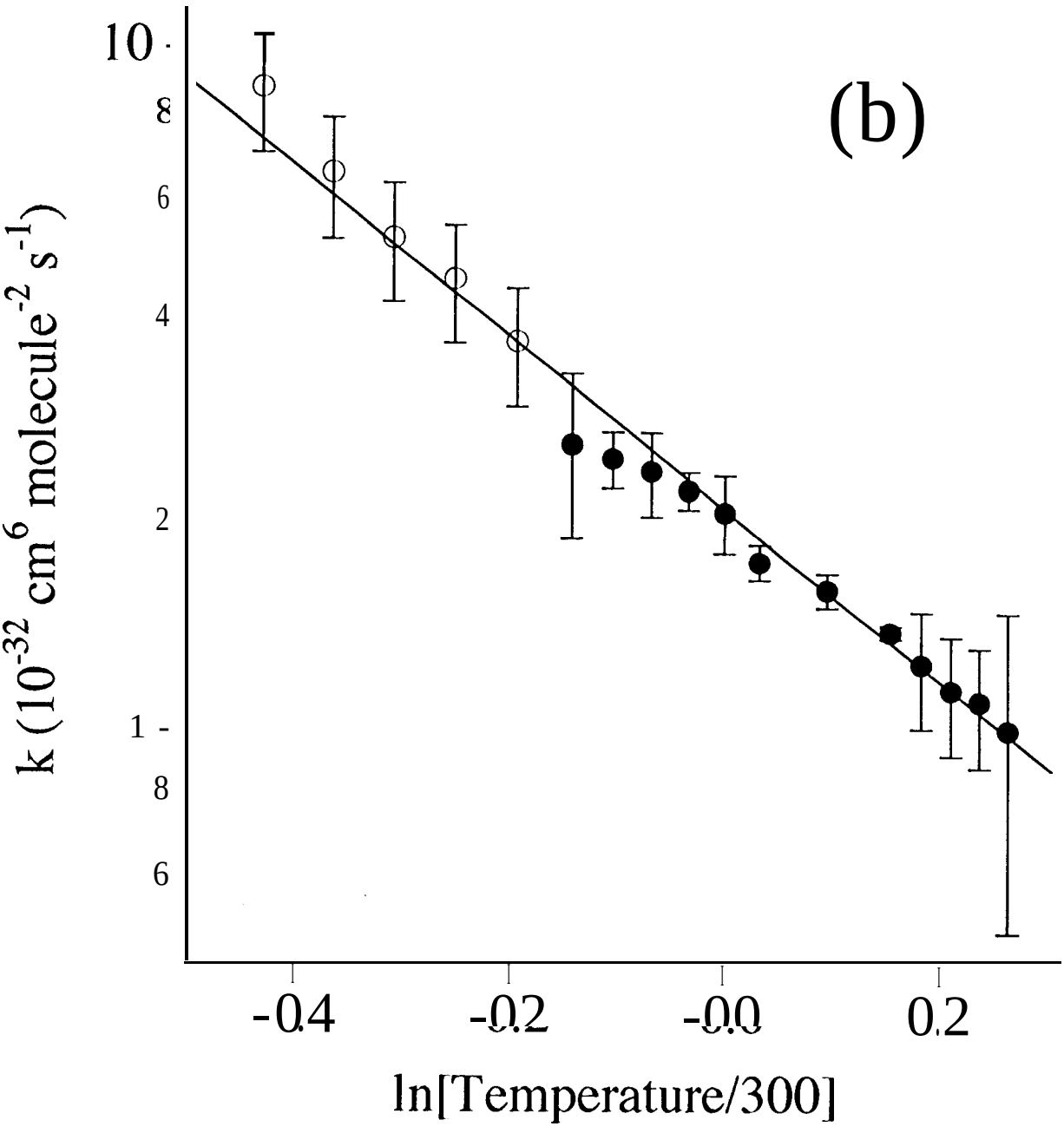
(b)
10
8
6
4
2
1
8
6
k (10^-32 cm^6 molecule^-2 s^-1)
-0.4
-0.2
-0.0
0.2
ln[Temperature/300]

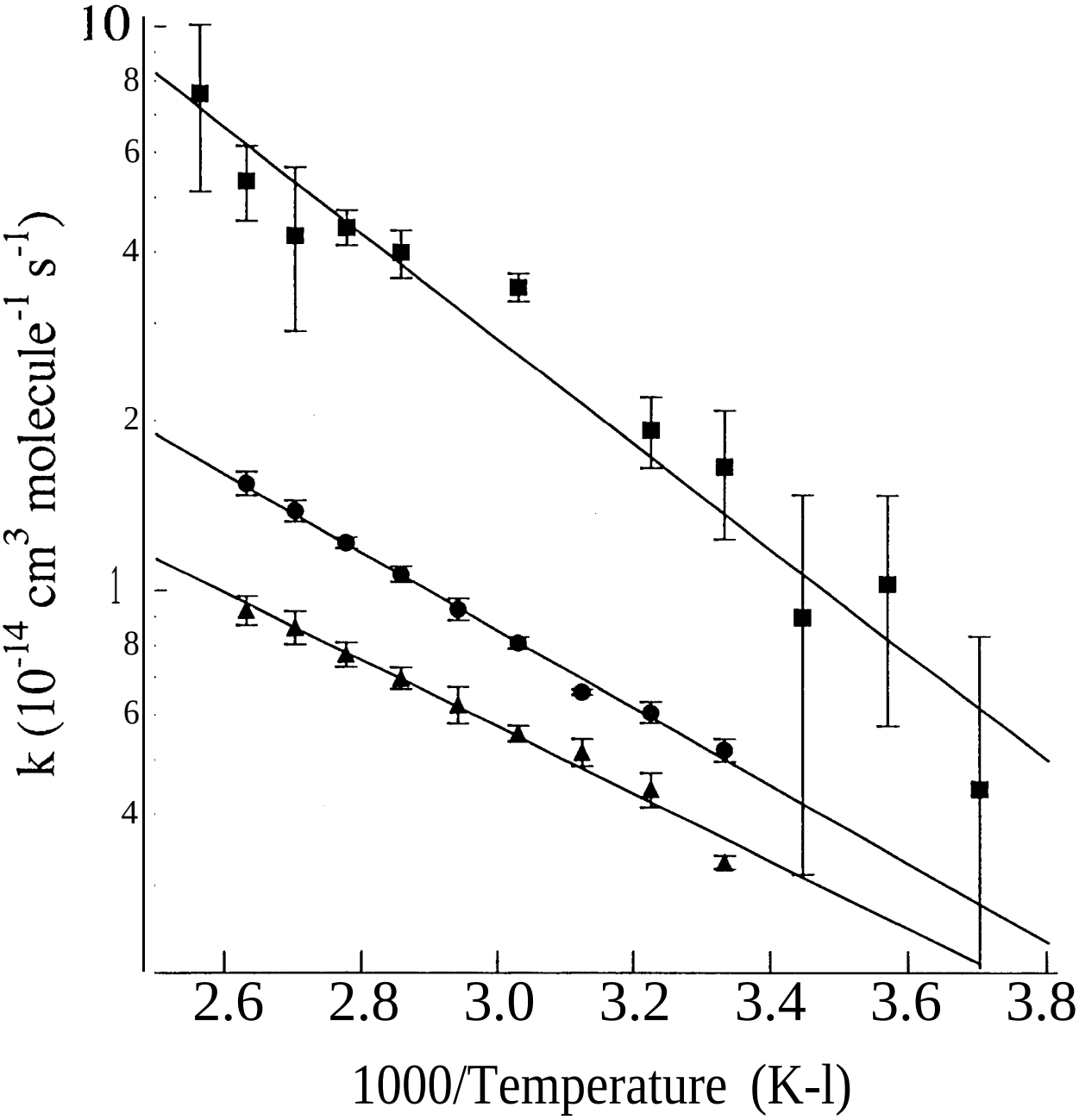
10
8
6
4
2
1
8
6
4
k (10-14 cm3 molecule-1 s-1)
2.6
2.8
3.0
3.2
3.4
3.6
3.8
1000/Temperature (K-l)

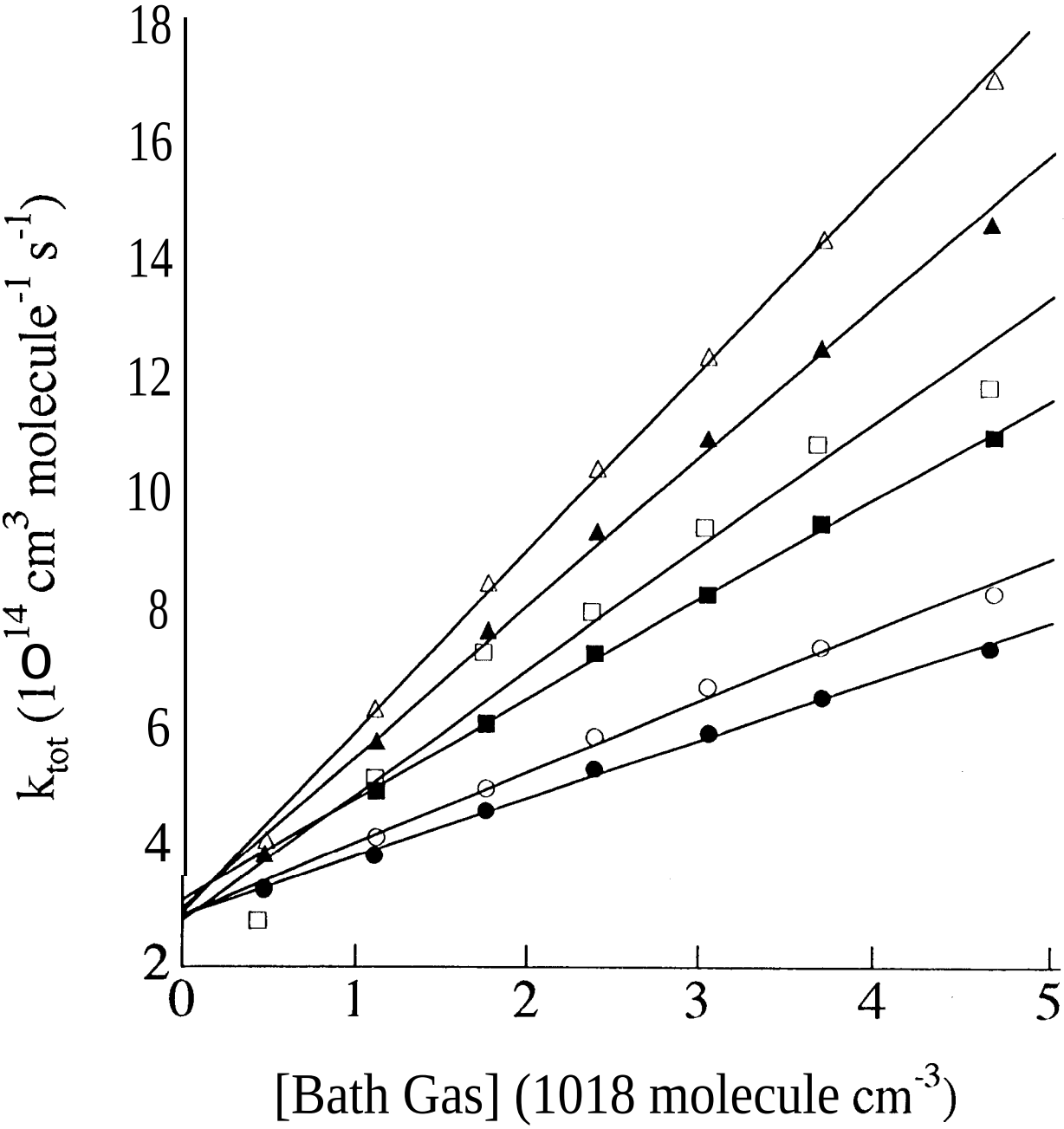
18
16
14
12
10
8
6
4
2
0
1
2
3
4
5
k_{tot} (10^{14} cm^3 $molecule^{-1}$ s^{-1})
[Bath Gas] (1018 molecule cm^{-3})

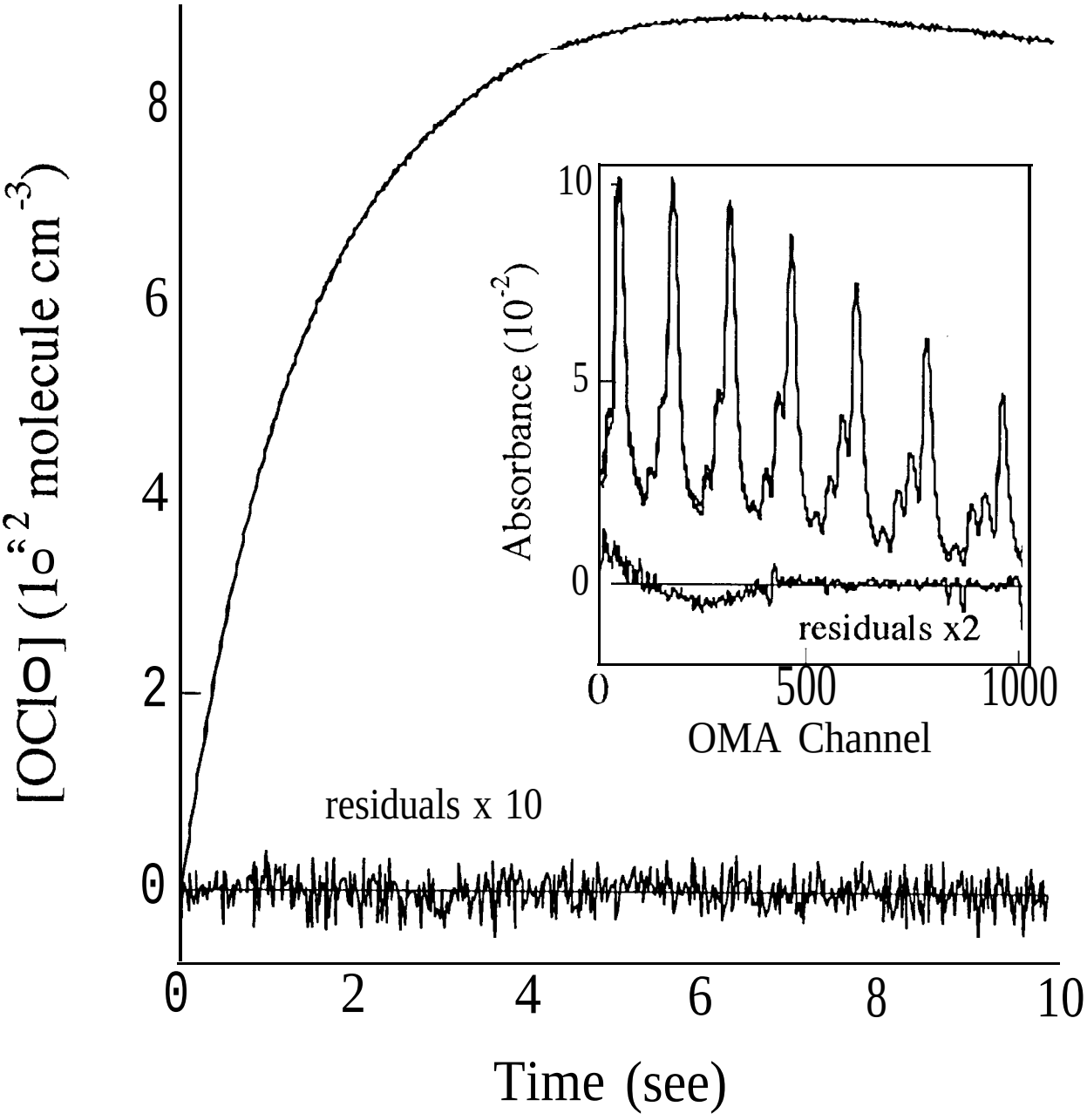
[OClO] (10^12 molecule cm^-3)
8
6
4
2
0
residuals x 10
0
2
4
6
8
10
Time (see)
Absorbance (10^-2)
10
5
0
residuals x2
0
500
1000
OMA Channel

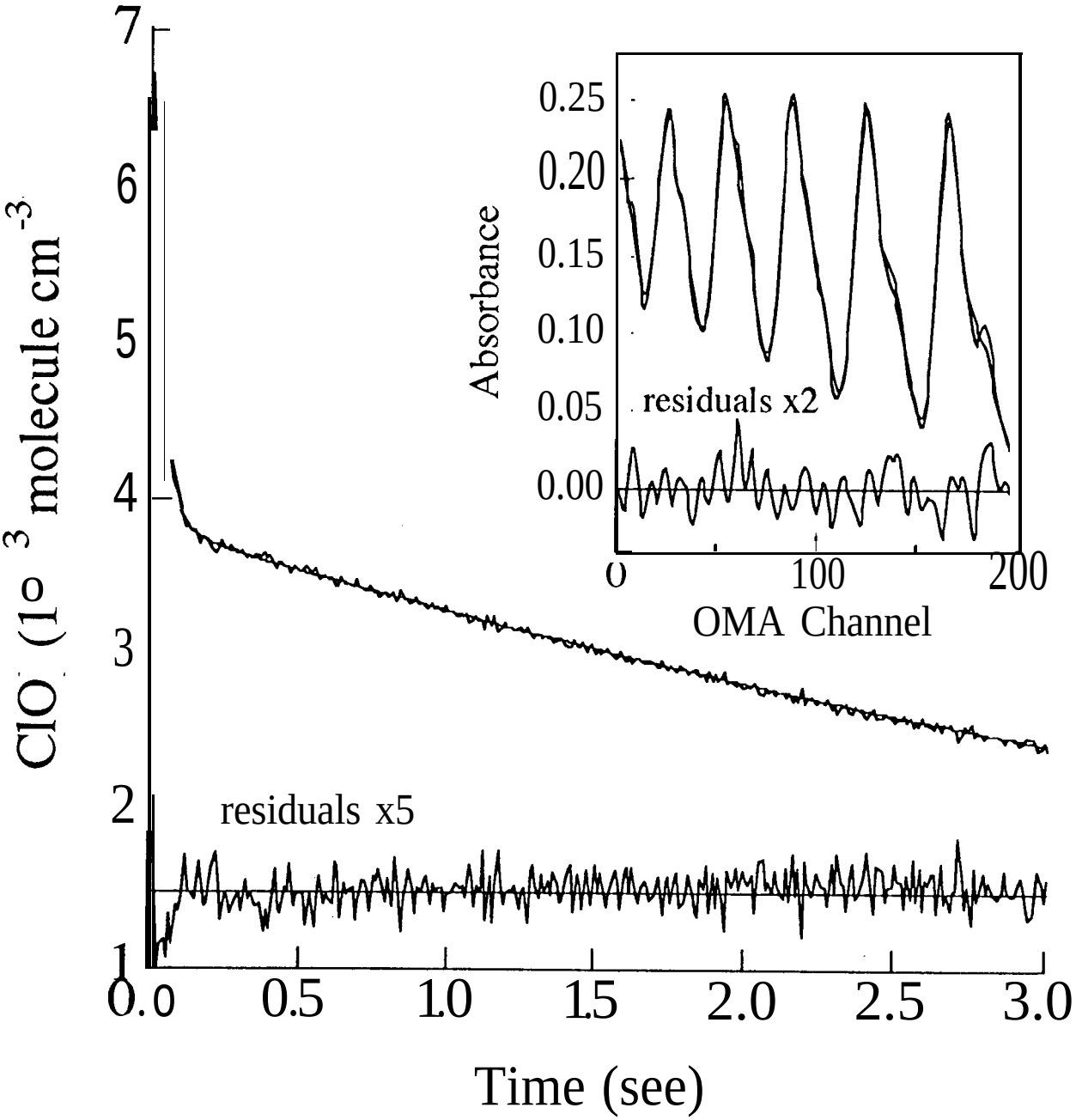
ClO (10^13 molecule cm^-3
7
6
5
4
3
2
1
0.0
0.5
1.0
1.5
2.0
2.5
3.0
Time (see)
residuals x5
Absorbance
0.25
0.20
0.15
0.10
0.05
0.00
residuals x2
0
100
200
OMA Channel

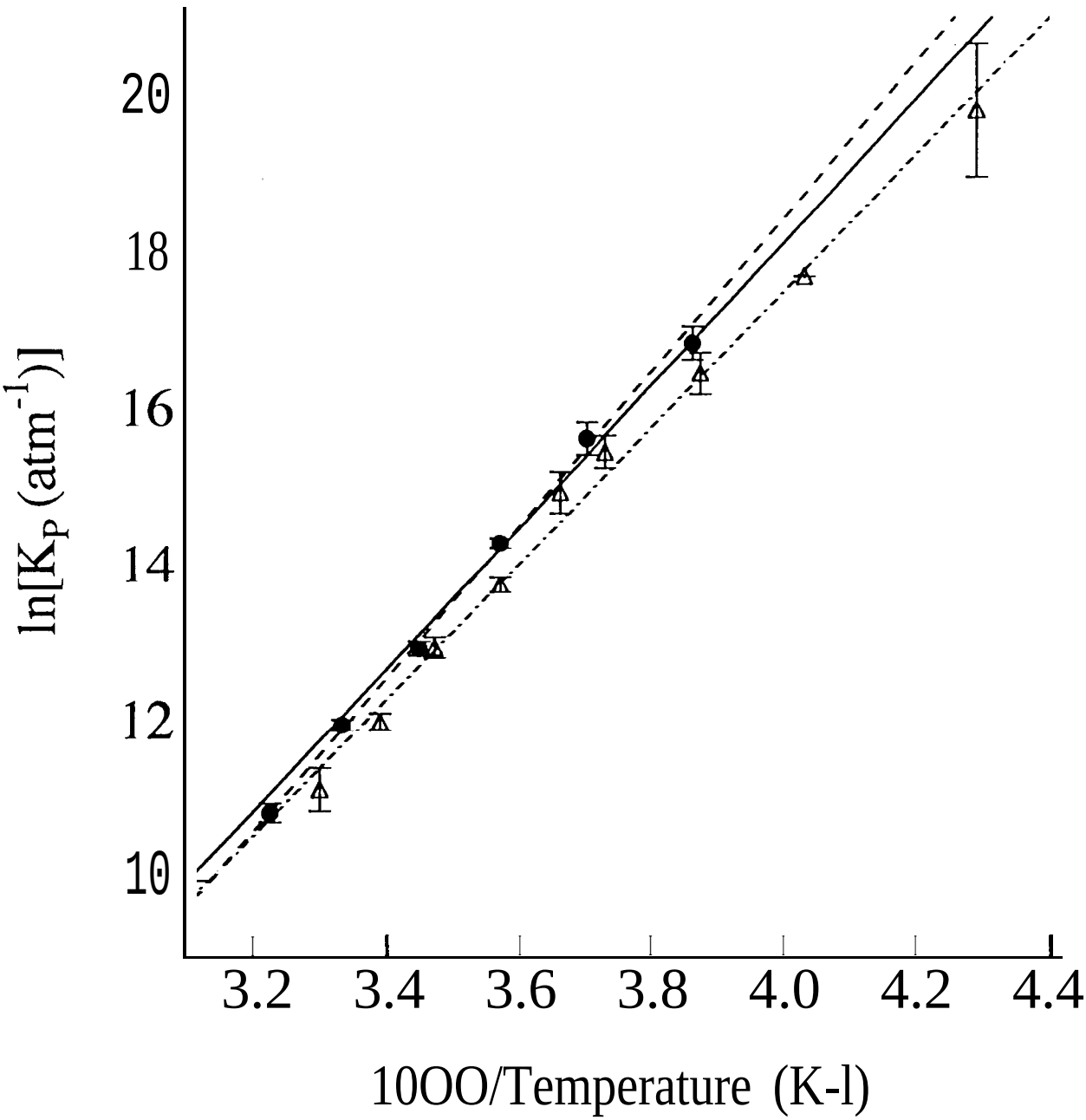
20
18
16
14
12
10
ln[K_P (atm^{-1})]
3.2
3.4
3.6
3.8
4.0
4.2
4.4
10OO/Temperature (K-l)

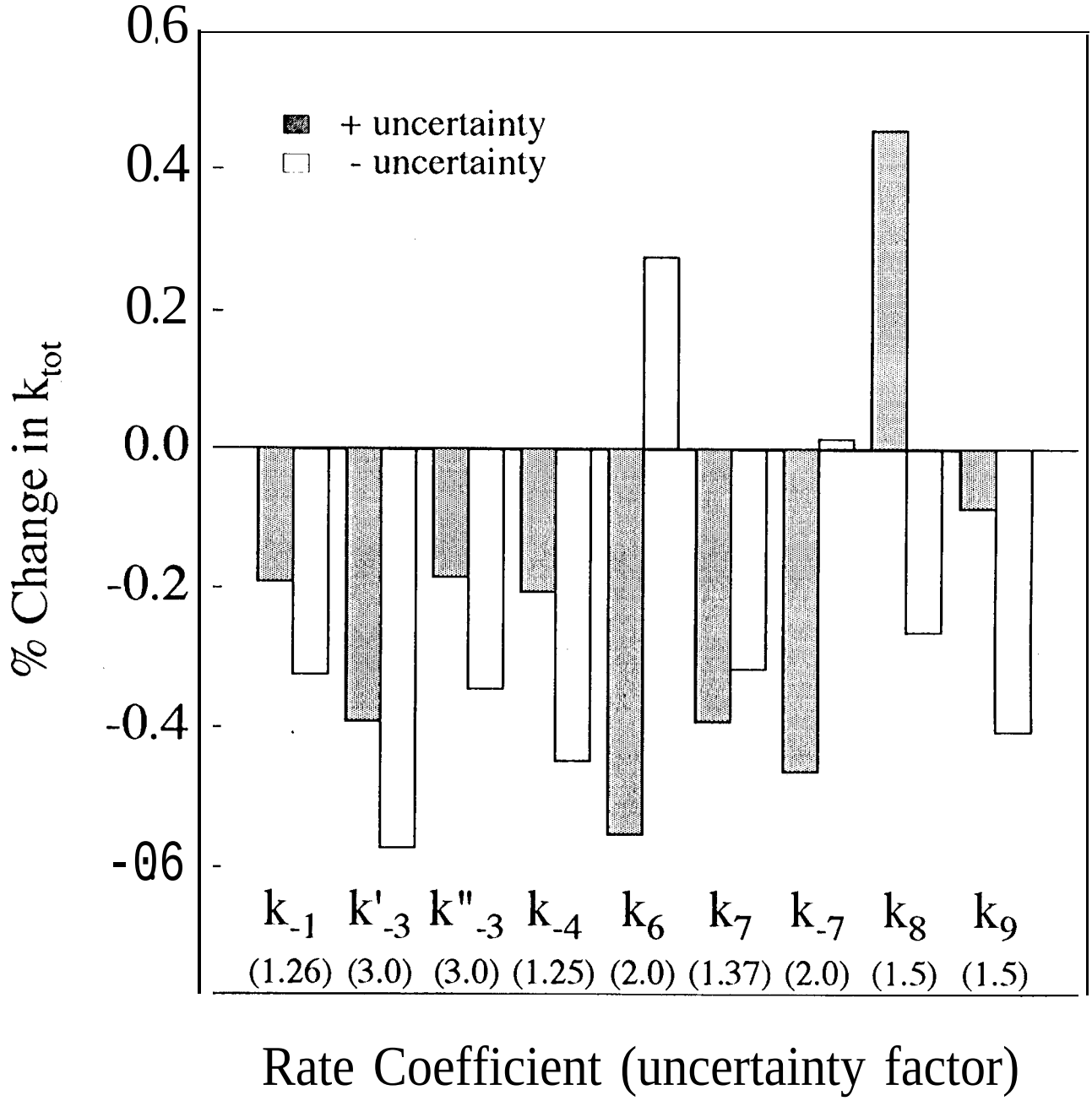
0.6
0.4
0.2
0.0
-0.2
-0.4
-06
+ uncertainty
- uncertainty
% Change in k_{tot}
k_{-1} (1.26)
k'_{-3} (3.0)
k''_{-3} (3.0)
k_{-4} (1.25)
k_6 (2.0)
k_7 (1.37)
k_{-7} (2.0)
k_8 (1.5)
k_9 (1.5)
Rate Coefficient (uncertainty factor)

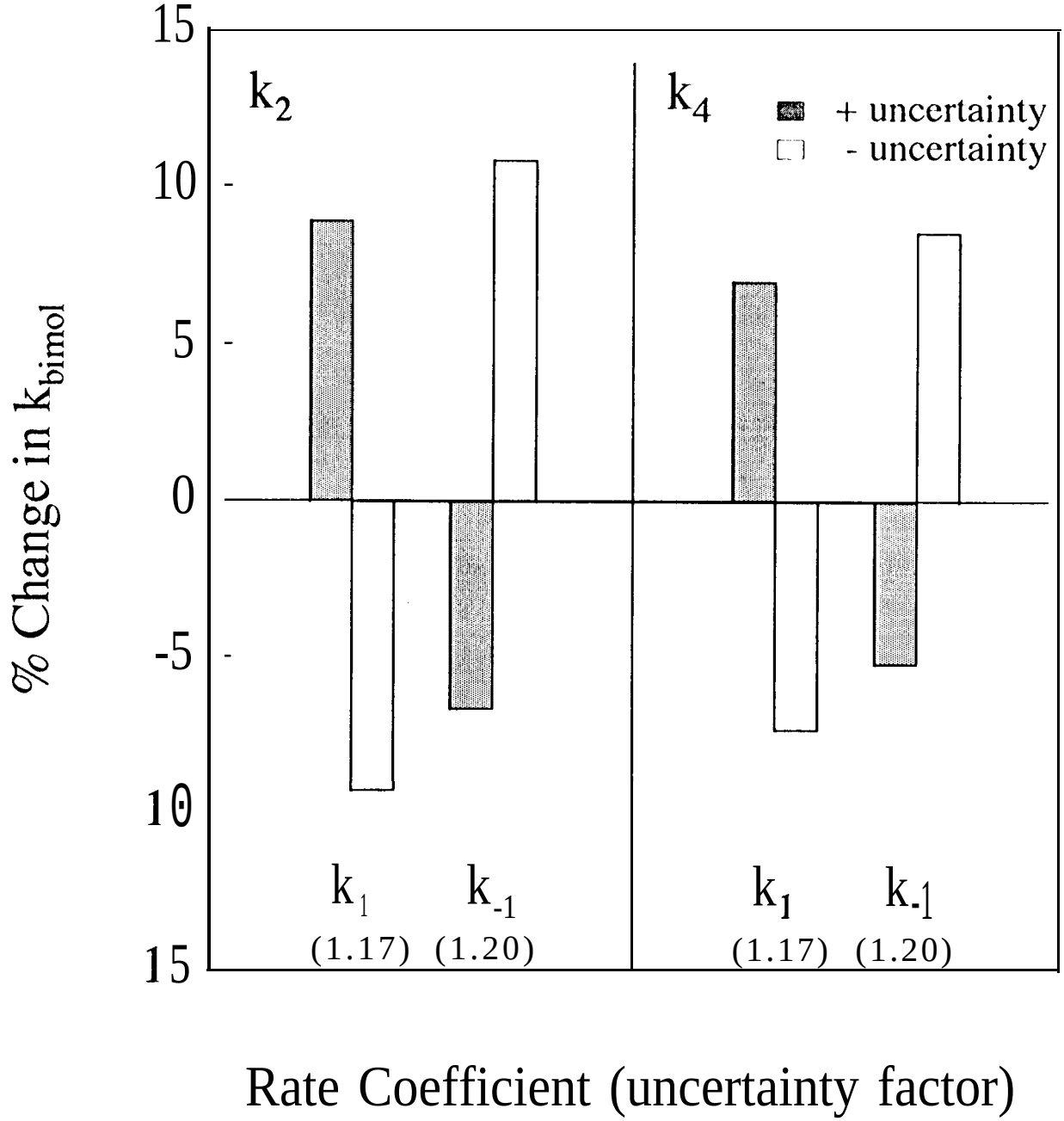
15
10
5
0
-5
10
15
% Change in k_{bimol}
k_2
k_4
+ uncertainty
- uncertainty
k_1 (1.17)
k_{-1} (1.20)
k_1 (1.17)
k_{-1} (1.20)
Rate Coefficient (uncertainty factor)

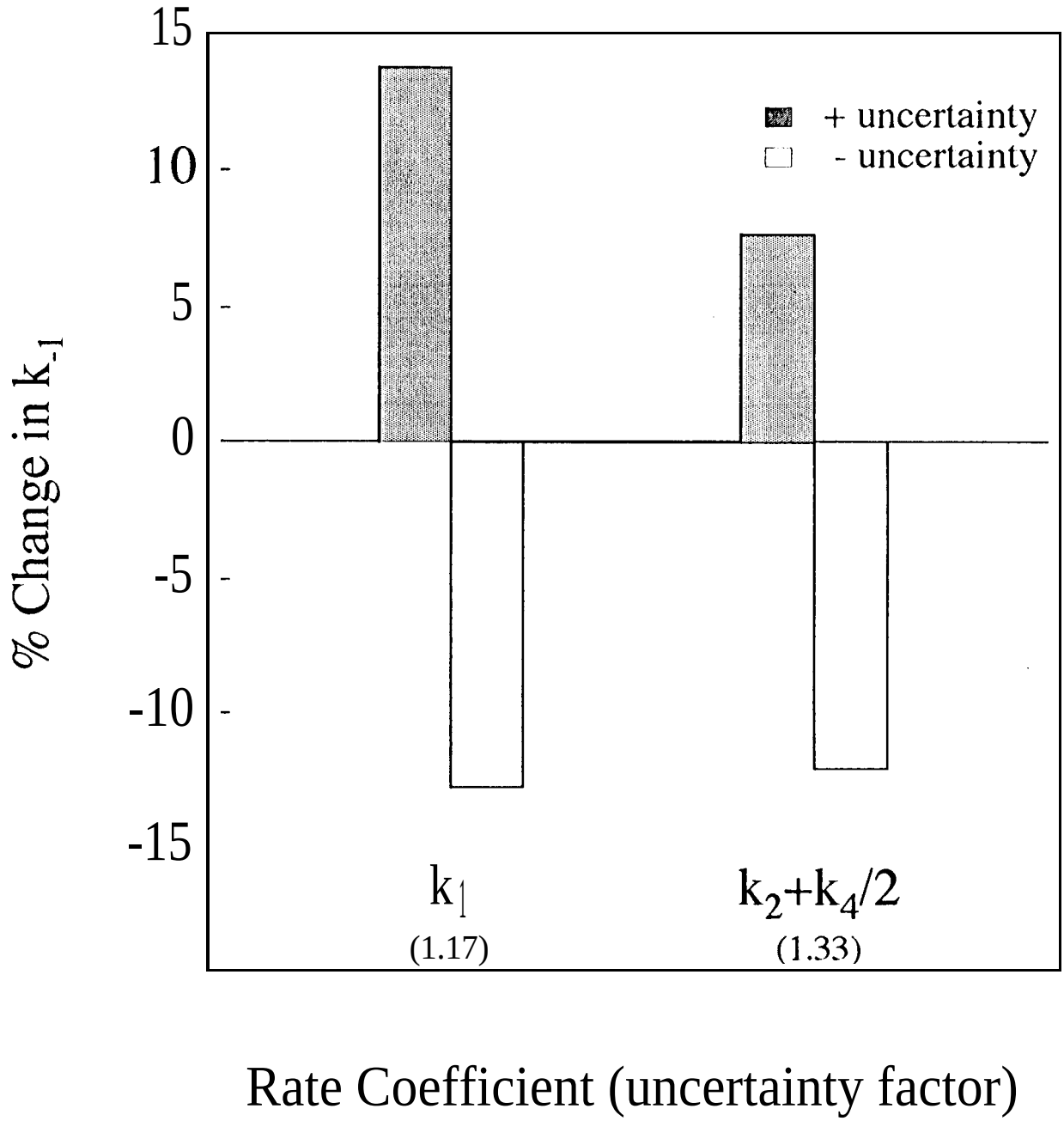
15
10
5
0
-5
-10
-15
% Change in k_{-1}
+ uncertainty
- uncertainty
k_1
(1.17)
$k_2+k_4/2$
(1.33)
Rate Coefficient (uncertainty factor)

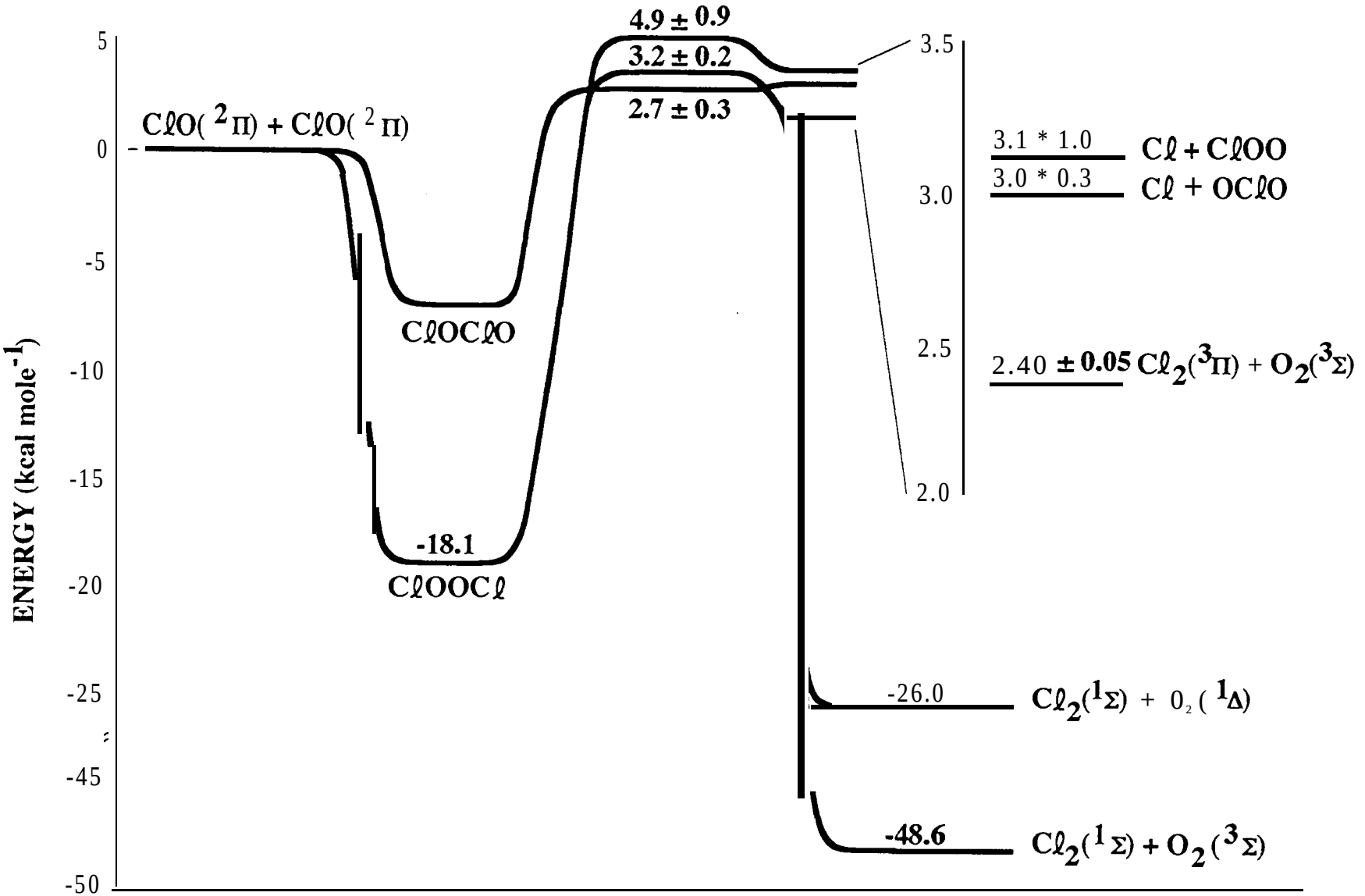
ENERGY (kcal mole-1)
5
0
-5
-10
-15
-20
-25
-45
-50
ClO(2Π) + ClO(2Π)
ClOOCl
-18.1
ClOCl
4.9 ± 0.9
3.2 ± 0.2
2.7 ± 0.3
3.5
3.0
2.5
2.0
3.1 * 1.0
Cl + ClOO
3.0 * 0.3
Cl + OClO
2.40 ± 0.05
Cl2(3Π) + O2(3Σ)
-26.0
Cl2(1Σ) + 02(1Δ)
-48.6
Cl2(1Σ) + O2 (3Σ)